Computer Modeling in
Engineering & Sciences

Tech Science Press

https://doi.org/10.32604/cmes.2026.083763

ARTICLE

Multi-Objective and Multi-Criteria Optimization of Energy Storage Planning in Renewable Distribution Networks

Alireza Norouzpour Shahrbejari[1], Nafiseh Pishbin[2], Mohammad Reza Maghami[3,*], Mazlan Mohamed[4,*] and Mohammad Golmohammad[1]

[1]Renewable Energy Department, Niroo Research Institute (NRI), Tehran, Iran
[2]Department of Electrical Engineering, Khatam University, 30 Hakim Azam Street, North Shiraz Avenue, Tehran, Iran
[3]Strategic Research Institute (SRI), Asia Pacific University of Technology and Innovation (APU), Kuala Lumpur, Malaysia
[4]Faculty of Artificial Intelligence and Cyber Security (FAIX), Universiti Teknikal Malaysia Melaka (UTeM), Melaka, Malaysia

*Corresponding Authors: Mohammad Reza Maghami. Email: Reza.maghami@apu.edu.my;
Mazlan Mohamed. Email: mazlan.mohamed@utem.edu.my

Received: 10 April 2026; Accepted: 19 May 2026; Published: 27 July 2026

ABSTRACT: This study presents a weighted-sum multi-criteria optimization framework using PSO for the optimal siting, sizing, and scenario-based operation of energy storage systems (ESSs) in renewable-integrated distribution networks. The proposed model concurrently addresses technical, economic, and reliability objectives—minimizing active power losses (PL), voltage deviation (VD), expected energy not supplied (EENS), and short-circuit level (SCL), while maximizing voltage sensitivity index (VSI) and power-loss sensitivity factor (PLSF). A Particle Swarm Optimization (PSO) algorithm with weighted-sum scalarization is employed to solve this complex, nonlinear optimization problem and effectively balance the conflicting operational goals. The framework is validated using IEEE 69-bus and IEEE 118-bus test systems under varying load conditions (20%, 50%, 100%, and 150%) with time-dependent photovoltaic (PV) and wind turbine (WT) generation profiles. Results demonstrate that the proposed approach achieves significant performance enhancements, reducing power losses by up to 54%, EENS by 88%, and operational cost by 22% while maintaining SCL values within protection limits. Furthermore, the inclusion of ESS units improves system reliability and voltage stability, ensuring smooth operation during load fluctuations and fault conditions. The findings confirm that the proposed weighted-sum multi-criteria optimization framework using PSO provides a scalable and protection-aware solution for integrating ESSs into renewable-rich distribution networks. It offers a robust planning and operational tool for next-generation smart grids, enabling a more efficient, resilient, and sustainable energy ecosystem.

KEYWORDS: Energy storage systems; multi-objective optimization; optimal placements; distribution networks; renewable integration; grid reliability

1 Introduction

In recent years, with the world moving towards renewable energy sources, smart distribution networks have undergone a significant transformation to enhance energy efficiency and reduce environmental emissions such as carbon dioxide. One of the key technologies powering this progress is energy storage systems (ESSs), which play a crucial role in increasing network flexibility, reliability, and economic efficiency while optimizing the utilization of distributed energy resources such as photovoltaics or wind, which will lead to instability in power generation. Furthermore, ESSs can help remove other negative effects of renewable-based distributed electricity generation, such as reverse power flow and energy loss [1].

ESS units reach peak effectiveness when optimally sited and assigned charge–discharge capacities, within a multi-objective framework. Such a multi-objective model can simultaneously minimize operating costs and power losses, enhance voltage stability, boost reliability, and preserve power quality. Using performance indices such as expected energy not supplied (EENS), voltage sensitivity index (VSI), and SCL to maintain network robustness, our approach further refines energy-storage management across diverse loading scenarios; ensuring that the batteries, together with distributed energy resources, improve power quality, raise reliability, and lower total system cost. While previous studies have addressed subsets of these objectives, this work contributes to the literature by simultaneously integrating all seven indices (PL, VD, EENS, VSI, PLSF, SCL, and operational cost) within a unified protection-aware framework for ESS planning. The main contribution of this study lies in the comprehensive problem formulation and the integration of technical, reliability, economic, and protection-related indices using existing optimization algorithms. The multi-objective framework defined by our objective functions is solved via an algorithm we develop in Section Mathematical Problem Formulations: "Mathematical Problem Formulations". This model is meticulously designed to integrate a diverse array of resources: from renewable energy sources like solar and wind to energy storage systems, while simultaneously considering multiple objective functions to reach an optimal solution in designing the studied networks. Contrary to earlier work, our algorithm finds the optimal number of ESSs, their position, and their capacity that produces the ideal designed model to simultaneously reach optimum technical, economical, and reliability factors.

1.1 Literature Review

The following section presents a detailed review of previous studies in this field, identifying existing research gaps and laying the foundation for the proposed comprehensive model. Research on optimizing the siting and sizing of ESS units in the presence of renewable energy sources has been extensively studied, yet key technical and economic markers remain inadequately addressed. Early reviews such as [2] focus on how ESSs can improve power reliability, but do not mention optimization strategies or multi-indicator assessment, which contribute a great deal to the deployment of an ideal design. To address these gaps, researchers in [3,4] used distributed renewable energy sources in their grid simulations and analysis, then suggested using ESS charge/discharge scheduling to minimize loss. VSI or reliability indices such as EENS were not addressed in their work; therefore, their work was not comprehensive enough. In [3] a genetic algorithm was used to adopt an optimal operation strategy which focuses on using grid-integrated battery ESS (BESS) coordinated with wind generation. Shao et al. studied cost reduction in ESSs by controlling the charge-discharge behavior in [4]. However, indices such as VSI and EENS have not been mentioned in either article. Researchers offering broader overviews, such as studies [5,6] have created different categories for ESS technologies based on their applications. In [6] the need for BESSs has been particularly discussed, an energy storage system focused on using electro-chemical batteries, in delivering multiple grid services. These reviews largely remained qualitative, lacking concrete optimization models. In contrast, Ref. [7] investigates changing load and photovoltaic panels' power to find multiple locations suitable for placing energy storage units with small changes in terms of ESS size. This assessment of voltage and loss impacts shows that location choices affect grid efficiency more than capacity alone.

Advanced planning models such as [8] address capital cost and voltage regulation in grids with large amounts of photovoltaic generation in existing practices that consider the needs of both distribution and transmission system operators, revealing economic and operational advantages. Meanwhile, Ref. [9] introduces a bi-level algorithm approach trying to find the optimal siting and management of ESSs, combining distributed generation and ESSs with uncertainty modeling, and yet falls short in incorporating the mentioned network performance metrics we consider in this paper. ESSs can have high capital costs;

therefore, Refs. [10,11] have tried to rationalize the use of these systems via revenue stacking, modeling frameworks to maximize profitability. These contributions define budget-constrained planning models for the optimal sizing and siting of ESSs as profit-generating assets that yield returns after a few years. Similarly, Ref. [12] explores demand-side management strategies of integrating ESSs into distribution networks from a policy and economic lens, but lacks granular modeling of network behavior. Another emerging trend with the rising use of distributed energy resources is community battery energy storage systems (C-BESS), as explored in [13], which proposes a multi-objective optimization model addressing minimizing VD and maximizing the utilization of distributed energy resources on the demand end. This study explains the conflict of interest between grid operators and prosumers (consumers who generate their own electricity), a theme absent in earlier centralized models, which is essential for decision-making.

Multi-objective optimization model of BESSs using evolutionary algorithms like the non-dominated sorting genetic algorithm-II is presented in [14], configuring cost, voltage fluctuation, and load fluctuation, to improve placement and sizing of BESSs. Degradation and its cost have been simplified and simulated in this study. Taking a step further, Ref. [15] incorporates uncertainty in unbalanced networks, using trade-off/risk analysis frameworks to identify reasonable solutions that remain effective when studying conflicting objectives and different indices. The most recent advancements are exemplified by [16], which proposes a two-level optimization model integrating ESS, demand-side management, photovoltaic, and electric vehicles. It leverages two-stage second-order cone programming to tackle the aforementioned complexities and presents an advanced smart distribution grid reconfiguration to reduce loss and stabilize voltage.

In 2024 and 2025, several studies improved the integration of renewable sources and their storage in multi-microgrid and reconfigurable networks. Ref. [17] experiment with battery/compressed air storage for the economic/flexibility scheduling of mixed (wind, PV, biomass)/non-renewable microgrids, which minimizes voltage security, energy loss, and costs under uncertainties using Unscented Transformation and hybrid grey wolf-red panda optimization, resulting in a 30%–60% cost reduction, a 46% loss/voltage drop reduction, a 10.55% security improvement, and 100% flexibility, but not including PLSF, EENS, and SCL. Ref. [18] developed a two-stage stochastic model for PV/wind generators with BESS in reconfigurable systems that have demand response, employing NSGA-II/MOPSO for a ten-year reduction of costs (44.87%), losses (63.65%), and voltage deviation (70.72%) on the IEEE 69-bus, thereby increasing renewable energy by 21.62%, yet disregarding VSI, EENS, and SCL. These studies stress the importance of flexibility/uncertainty handling but provide only partial indices, which means that there is a requirement for unified frameworks. Ref. [19] obtains the optimal location of BESS in PV/wind RDSs using a multi-objective approach by reducing losses/PSI and increasing VSI through probabilistic/PMR and IGWO-TOPSIS on IEEE 33/94-bus, obtaining distributed BESS loss reduction, still neglecting VD, EENS, SCL, and CM. Ref. [20] suggests the cluster-based multi-layer optimization technique for DES in the PV grid that reduces cost/loss and increases the voltage level through iterative layers over IEEE-118, saving ES cost by 22.88%/losses by 9.60%/fluctuations by 8.60%, but leaving PLSF, VSI, EENS, and SCL out. Such works expose uncertainties/clustering but they operate with only limited indices, thus it is necessary to have unified models. Much research on dynamic grids has been published; however, several issues remain unaddressed. For instance, many models overlook key technical indicators such as VSI, EENS, or SCL; few simultaneously address degradation, reliability, power quality, and cost in a unified framework; and only limited studies consider operational uncertainty alongside grid-level performance metrics. A comprehensive review of the literature (summarized in Table 1) reveals a clear research gap: while previous studies have addressed 3 to 6 of the seven key indices considered in this work, none have simultaneously optimized all seven indices (PL, VD, EENS, VSI, PLSF, SCL, and operational cost) within a unified protection-aware framework under multiple loading scenarios with time-dependent PV and WT generation. This study fills that gap by developing a comprehensive multi-objective optimization model that integrates technical, reliability, and protection objectives in a single optimization environment. Recent studies such as [21] focused on BESS placement under PV deployment uncertainty but omitted EENS and SCL. Ref. [22] introduced fairness metrics but did not consider EENS or SCL. Ref. [23] provided a practical BESS allocation study but lacked EENS, SCL, PLSF, or VSI. Ref. [24] considered only three objectives (loss, voltage deviation, PV consumption). Ref. [25] focused solely on BESS without considering PV/WT uncertainties or protection constraints. Ref. [26] conducted a statistical comparison but did not include EENS, SCL, PLSF, or VSI. Ref. [27] proposed an MGNDO (Multi-objective Generalized Normal Distribution Optimization) algorithm but lacked voltage deviation and protection-related indices. Ref. [28] developed a bi-level planning model but omitted EENS, SCL, and PLSF. Ref. [29] incorporated VSI but not EENS or SCL. Refs. [30,31] focused on peak demand reduction and congestion mitigation, respectively, both lacking reliability and protection indices. Furthermore, Ref. [32] addressed battery balancing with SOC estimation, while Ref. [33] recently developed a hybrid GRU-classical optimization method for optimal sizing and placement of synchronous condensers to enhance system strength and reliability in renewable-based weak grids. The present study extends this research direction by proposing a comprehensive seven-objective, protection-aware framework for ESS planning under multiple loading scenarios.

Table 1: Side-by-side comparison of the proposed framework to prior approaches.

	PV	WT	ESS	Power Flow	Grid Connect	Multi-Objective Function						
						VD	PLSF	PL or EL	VSI	EENS	SCL	CM
[2]	✗	✗	✓	✓	✓	✗	✗	✗	✗	✓	✗	✓
[3]	✗	✓	✓	✓	✓	✗	✗	✓	✗	✗	✗	✓
[4]	✗	✓	✓	✓	✓	✗	✗	✓	✗	✗	✗	✓
[5]	✗	✓	✓	✓	✓	✗	✗	✓	✗	✓	✗	✓
[6]	✓	✓	✓	✓	✓	✓	✗	✓	✓	✗	✗	✓
[7]	✓	✗	✓	✓	✓	✓	✗	✓	✗	✗	✗	✓
[8]	✓	✗	✓	✓	✓	✓	✗	✓	✓	✓	✗	✓
[9]	✓	✓	✓	✓	✓	✓	✗	✓	✓	✓	✗	✓
[10]	✓	✗	✓	✓	✓	✓	✗	✓	✓	✗	✗	✓
[11]	✓	✓	✓	✓	✓	✓	✗	✓	✗	✗	✗	✓
[12]	✓	✓	✓	✓	✓	✗	✗	✓	✗	✗	✗	✓
[13]	✓	✗	✓	✓	✓	✓	✗	✓	✗	✗	✗	✓
[14]	✓	✓	✓	✓	✓	✓	✗	✓	✓	✗	✗	✓
[15]	✓	✗	✓	✓	✓	✓	✗	✓	✗	✓	✗	✓
[16]	✓	✓	✓	✓	✓	✓	✗	✓	✓	✗	✗	✓
[17]	✓	✓	✓	✓	✓	✓	✗	✓	✓	✗	✗	✓
[18]	✓	✓	✓	✓	✓	✓	✗	✓	✗	✗	✗	✓
[19]	✓	✓	✓	✓	✓	✗	✗	✓	✓	✗	✗	✓
[20]	✗	✓	✓	✓	✓	✓	✗	✓	✗	✗	✗	✓
[21]	✓	✗	✓	✓	✓	✓	✗	✓	✗	✗	✗	✗
[22]	✓	✗	✓	✓	✓	✓	✗	✓	✗	✗	✗	✗
[23]	✓	✗	✓	✓	✓	✓	✗	✓	✗	✗	✗	✗
[24]	✓	✗	✓	✓	✓	✓	✗	✓	✗	✗	✗	✓
[25]	✓	✗	✓	✓	✓	✓	✗	✓	✗	✗	✗	✓
[26]	✓	✗	✓	✓	✓	✓	✗	✓	✗	✗	✗	✓

(Continued)

Table 1 (continued)

	PV	WT	ESS	Power Flow	Grid Connect	Multi-Objective Function						
						VD	PLSF	PL or EL	VSI	EENS	SCL	CM
[27]	✓	✓	✓	✓	✓	✗	✗	✓	✗	✗	✗	✓
[28]	✓	✓	✓	✓	✓	✓	✗	✓	✗	✗	✗	✓
[29]	✓	✗	✓	✓	✓	✓	✗	✓	✓	✗	✗	✓
[30]	✓	✗	✓	✓	✓	✓	✗	✓	✗	✗	✗	✗
[31]	✓	✗	✓	✓	✓	✓	✗	✓	✓	✗	✗	✗
This study	✓	✓	✓	✓	✓	✓	✓	✓	✓	✓	✓	✓

Note: WT = Wind turbine, PV = Photovoltaic, ESS = Energy storage system, VD = Voltage deviation, PLSF = Power loss sensitivity factor, PL = Power losses, EL = Energy losses, VSI = Voltage stability index, EENS = Expected energy not served, SCL = Short circuit level, CM = Cost minimization.

1.2 Research Problem and Gaps

The increasing penetration of renewable energy resources such as PV and WT systems introduces significant variability and uncertainty in power generation, which complicates the operation and planning of modern distribution networks. Although the integration of energy storage systems (ESS) has emerged as an effective solution to mitigate these challenges, the optimal siting, sizing, and scheduling of ESS remains a complex, multi-dimensional problem involving both technical and economic trade-offs. Most existing studies on ESS allocation in distribution networks have primarily focused on minimizing active power losses and voltage deviation, often neglecting the broader system impacts such as reliability, voltage stability, and protection coordination. For instance, while several works have addressed energy storage for loss minimization or cost reduction, they typically omit reliability indices such as the Expected Energy Not Supplied (EENS), which directly reflect the continuity of power supply. Similarly, short-circuit level (SCL) constraints—which are critical for ensuring that system upgrades do not violate protection device ratings—are rarely incorporated into the optimization process. Consequently, many existing frameworks produce technically efficient but protection-infeasible solutions.

Moreover, most prior research treats ESS operation as a static planning problem, ignoring the dynamic interactions between hourly renewable generation profiles, load variations, and SOC constraints. The absence of time-coupled scheduling often leads to suboptimal energy exchange between the grid and the storage system, thereby reducing the operational efficiency and cost-effectiveness of ESS deployment. In addition, comprehensive multi-objective formulations that jointly address PL, VD, EENS, stability indices (VSI and PLSF), SCL, and total operational cost are scarce in the literature. Existing approaches tend to optimize a limited subset of these indices, leading to solutions that enhance one performance metric at the expense of another. Furthermore, comparative assessments of metaheuristic optimization techniques, such as PSO, GA, and Simulated Annealing (SA), under identical system conditions are limited, leaving uncertainty regarding the most effective algorithm for ESS planning in renewable-rich distribution systems. Table 1 comparing the recent study based on different objectives.

Table 1 provides a side-by-side comparison of the proposed framework with 20 recent studies. The check marks (✓) and crosses (✗) indicate whether each study considered the corresponding index or component. The proposed work is the only one that simultaneously addresses all seven key indices (VD, PLSF, PL, VSI, EENS, SCL, and CM) while incorporating both PV and WT generation under multiple loading scenarios.

A comprehensive review of the literature (Table 1) reveals a critical research gap: while numerous studies have made significant contributions to ESS planning, none of the existing works simultaneously address all seven key performance indices (PL, VD, EENS, VSI, PLSF, SCL, and operational cost) in a unified framework. In contrast, the proposed framework uniquely contributes to the literature by simultaneously optimizing these seven indices—active power losses (PL), voltage deviation (VD), EENS, voltage stability index (VSI), PLSF, short-circuit level (SCL), and total operational cost—within a unified multi-objective optimization model. The methodological novelty lies in the protection-aware formulation that explicitly incorporates SCL (to minimize disruption to protection coordination) and PLSF for accurate siting, alongside the other indices, under multiple realistic loading scenarios (20%, 50%, 100%, and 150% of nominal load) with time-dependent PV and WT generation profiles. The framework is validated on IEEE 69-bus and IEEE 118-bus test systems, demonstrating significant performance enhancements including up to 54% reduction in power losses, 88% reduction in EENS, and 22% reduction in operational cost, while maintaining SCL values within protection limits. This holistic and protection-aware optimization framework provides a more realistic and robust solution for ESS planning in renewable-rich distribution networks, effectively filling the critical research gaps identified in the literature.

1.3 Research Aim and Objectives

The primary aim of this research is to develop a comprehensive weighted-sum multi-criteria optimization framework using PSO for the optimal siting, sizing, and scenario-based scheduling of ESS in renewable-integrated distribution networks. The proposed multi-criteria optimization framework simultaneously optimizes technical, economic, and protection-related performance indicators, ensuring that the coordinated operation of ESS, PV, and wind turbine (WT) sources enhances efficiency, reliability, and voltage stability without violating SCL or protection constraints. To achieve this aim, the study pursues the following objectives:

- Formulate a comprehensive multi-objective optimization problem that integrates seven key performance indices—active PL, VD, EENS, VSI, PLSF, SCL, and total operational cost—representing the combined technical, reliability, and economic dimensions of ESS planning.
- Develop a protection-aware multi-criteria optimization formulation that enforces SCL limits and ensures coordination with existing protection devices, preventing over-current or equipment-rating violations during fault conditions.
- Incorporate operational constraints by integrating renewable generation profiles (PV and WT) and ESS SOC dynamics under four representative loading scenarios (20%, 50%, 100%, and 150% of nominal load), ensuring realistic scenario-based planning and dispatch decisions.
- Implement a PSO-based multi-criteria optimization algorithm using weighted-sum scalarization to generate high-quality solutions that reveal the trade-offs among competing objectives, and compare its performance against GA and SA in terms of convergence rate, solution diversity, and computational efficiency.
- Validate the proposed framework on benchmark IEEE 69-bus and IEEE 118-bus distribution systems under multiple loading conditions (20%, 50%, 100%, and 150%), quantifying improvements in technical indices, reliability measures, and total cost relative to baseline and competing methods.
- Perform sensitivity and robustness analyses on the multi-criteria optimization weighting factors to evaluate the stability of ESS placement and scheduling decisions under varying system conditions.

This research contributes to the literature in the following aspects:

- A comprehensive seven-objective optimization framework that simultaneously integrates active power losses, voltage deviation, expected energy not supplied, voltage stability index, power loss sensitivity

factor, short-circuit level, and operational cost a combination that has received limited attention in previous ESS planning studies.
- A protection-aware formulation that explicitly incorporates short-circuit level constraints to ensure coordination with existing protection devices.
- Comprehensive validation on both IEEE 69-bus and IEEE 118-bus systems under four realistic loading scenarios (20%–150%) with time-dependent PV and WT generation profiles.
- A systematic sensitivity analysis on weighting factors to demonstrate the robustness of the obtained ESS placement and sizing decisions.

The proposed framework provides high-quality compromise solutions for ESS allocation through standard weighted-sum scalarization within PSO, effectively balancing the seven techno-economic-reliability objectives and offering a practical decision-support tool for utilities and system operators in renewable-dominated smart grids. In order to fill the gaps identified in earlier research, this work achieves a full optimization model that positions desired ESS units in distribution networks while simultaneously achieving technical, economic, and reliability goals. These are the main contributions.

- A comprehensive multi-objective framework is proposed that determines the optimal number, location, and capacity of ESS units by balancing operational costs, power losses, voltage stability, network reliability, and power quality, while ensuring minimal disruption to protective configurations and system fault levels.
- Technical and economic interactions between ESS integration and distributed energy resources are analyzed, emphasizing the important role they have in improving system stability and optimizing grid operation under diverse load conditions.
- Reliability and power quality indices, such as EENS, VSI, SCL, and power loss minimization, are incorporated in the study which directly influences network performance and resilience.
- The stored energy within ESSs is managed so that both technical constraints and economic objectives are met, and energy storage is optimized under different loading scenarios.

This article is ordered in five sections. Section 1 introduces the importance of studying all seven objective functions at the same time to be able to make the best possible decision as to the placement of ESSs in our distribution network. Section 2 discusses the method used to reach the best model that includes distributed sources while studying how the placement of ESSs influences the grid. In Section 3 we show the algorithm that was developed to efficiently manage the model. Objective functions used in the algorithm are explored mathematically. Section 4 outlines the main results from the simulated scenarios and discusses their findings. Section 5 concludes the article and its results.

2 Research Methodology

This section presents the proposed conceptual framework for determining the optimal siting, sizing, and scheduling of energy storage systems (ESS) in distribution networks with integrated distributed energy resources (DERs). The research methodology is structured into three main components: the conceptual multi-objective optimization framework and data flow, the mathematical problem formulation with system constraints, and the multi-objective optimization algorithm design and solution procedure. Together, these components establish a comprehensive and protection-aware approach for ESS planning that simultaneously addresses technical, economic, and reliability objectives. As illustrated in Fig. 1, the proposed framework connects distributed generation (DG) units—specifically photovoltaic (PV) and wind turbine (WT) systems—with energy storage systems through a hierarchical control structure managed by a central controller. This configuration enables the coordination of real-time operational data with long-term planning decisions, ensuring efficient and stable system performance. The model determines the optimal number, location, and capacity of ESS units through a multi-objective decision process aimed at enhancing the grid's overall efficiency, reliability, and power quality.

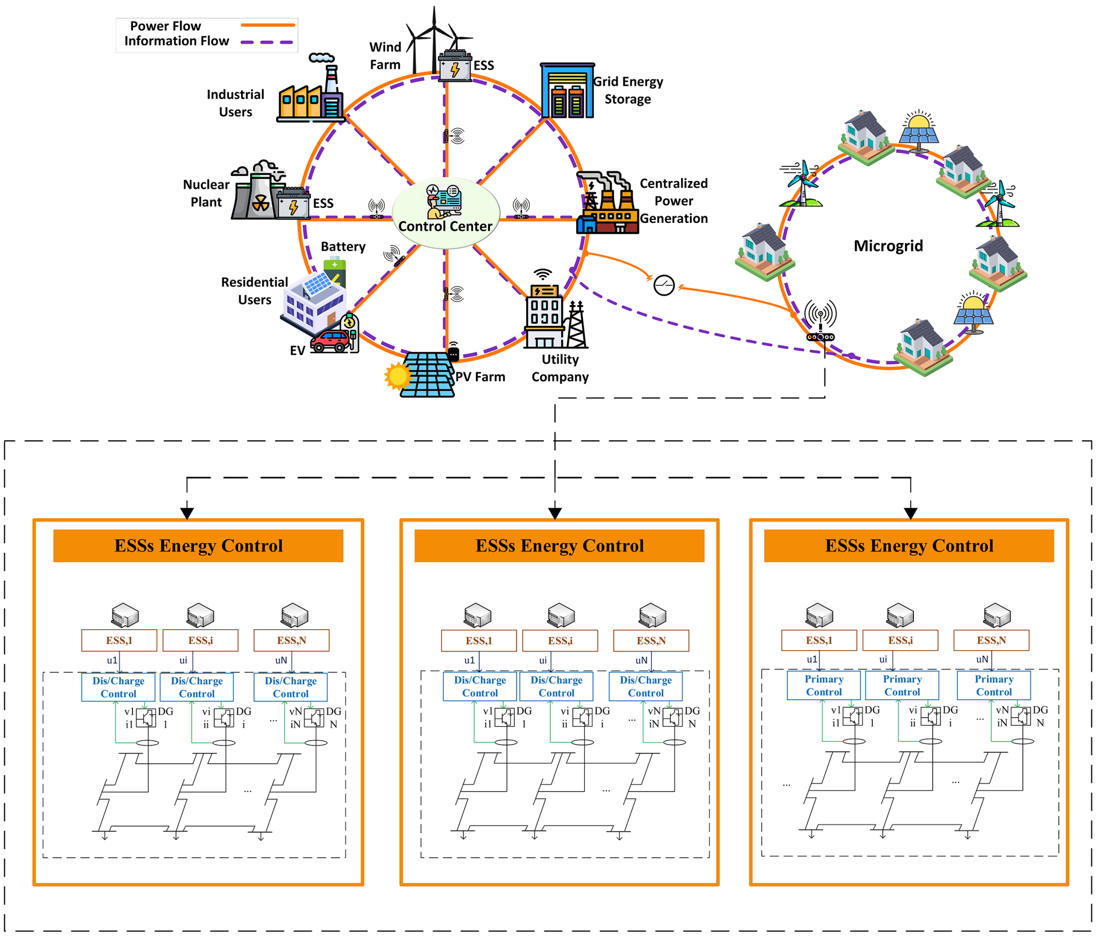

Figure 1: Schematic overview of the proposed multi-objective ESS siting and sizing framework.

The framework simultaneously optimizes seven critical performance indices: active power loss (PL), voltage deviation (VD), expected energy not supplied (EENS), voltage stability index (VSI), power-loss sensitivity factor (PLSF), short-circuit level (SCL), and total operational cost. These indices are used to balance competing technical and economic factors—such as maintaining high power quality, minimizing system losses, ensuring reliable generation, and controlling fault current levels within protection limits. To address the nonlinear and multi-criteria nature of this optimization problem, a standard Particle Swarm Optimization (PSO) algorithm with weighted-sum scalarization is employed. The approach efficiently explores the solution space and identifies high-quality solutions that achieve an effective trade-off between cost, reliability, and technical performance. This algorithm operates within the hierarchical control framework to prevent operational disruptions and to maintain power quality under variable renewable generation and loading conditions.

Finally, the proposed framework is evaluated under multiple loading scenarios (20%, 50%, 100%, and 150% of nominal demand) to assess its flexibility and robustness. By addressing the limitations highlighted in Section 1.2, this model integrates factors often overlooked in previous studies—such as short-circuit level management, reliability improvement, and cost minimization—ensuring that ESS units are deployed in configurations that deliver a reliable, low-loss, and economically efficient distribution network.

Mathematical Problem Formulations

Herein, we explain the algorithm developed for the proposed conceptual model that helps create an efficient and reliable management system. The optimization process of this multi-objective algorithm takes a number of technical and operational parameters into account, such as hourly load profiles, real-time electricity prices, photovoltaic and wind turbine generation, and the initial setup of the IEEE 69-bus distribution network. The objective is to minimize total generation cost and system losses while maximizing power quality and system stability. A Hierarchical Control System is utilized to effectively manage the coordination between distributed generators, energy storage units, and the central grid. This system is structured in three levels:

- **Primary control** manages voltage and frequency in real time at the local level.
- **Secondary control** provides coordination among distributed sources and utility sources to enhance overall performance.
- **Tertiary control** deals with energy dispatch, optimal siting and sizing of ESS units, and system-wide energy balancing.

This hierarchical control enhances the flexibility and resilience of the distribution network in response to varying load and generation conditions. The optimization process is performed for different load levels corresponding to 20%, 50%, 100%, and 150% of the nominal system load, to evaluate the impact of ESSs placement across a wide range of operating scenarios. Key technical indices used in the objective function include Active Power Loss (PL), Voltage Deviation (VD), Expected Energy Not Supplied (EENS), Voltage Stability Index (VSI), Power Load Sensitivity Factor (PLSF), Short Circuit Level (SCL), and State of Charge (SOC) of ESS units. These indices reflect the real-time status of the system and are critical to guiding the optimization process in making informed decisions for ESS planning. Algorithm 1, with its flowchart depicted in Fig. 2 provides a structured step-by-step framework to identify the most effective ESS siting and sizing configuration across the network, based on the proposed multi-objective model.

Algorithm 1: Step-by-step process flowchart for the suggested multi-objective framework for the placement of ESSs

---

Start

Load Profile ($L(t)$) **% *Load Profile and Parameters***

- Electricity Price $\mathrm{CE}(t)$ = Get Electricity Price (t)
- Initial_ Reconfiguration κ_0 = Get Initial Reconfiguration $(\mathcal{G})$
- Initial_ DG_ Generation $P_{\mathrm{DG}}{}^{0}(t)$ = G8et Initial DG (PV (t), WT(t))

Step 1: Calling and Calculating Required Parameters for Optimal Placement of ESSs

- Calculate Required Parameters $(L(t), \mathrm{CE}(t), \kappa_0, P_{\mathrm{DG}}{}^{0}(t), \theta_{\mathrm{CE}})$

  if Electricity Price $\mathrm{CE}(t)$ > Threshold θ_{CE}:

  Adjust Load Profile $(L(t), \mathrm{CE}(t))$

  else:

- Maintain Current Profile $(L(t))$

(Continued)

Algorithm 1 (continued)

Step 2: Initialize Hierarchical Control System

- Initialize and Implement Hierarchical Control System (Primary, Secondary, Tertiary)
- Import Network Data for each system (Bus and Line Information)

Step 3: Calculate the Initial Techno-Economic Indices of the Power System

- → Run power flow to calculate:
- Initial Power Losses (PL)
- Initial Voltage Deviation (VD)
- Initial Expected Energy Not Supplied (EENS)
- Initial Voltage Stability Index (VSI)
- Initial Power Loss Sensitivity Factor (PLSF)
- Initial Short Circuit Level (SCL)
- Initial State of Charge (SOC) of ESS
- Initial DG Operating Limits

Step 4: Call the Multi-Objective Optimization Framework

- Define objective functions and technical constraints
- Initialize Optimization Algorithm (PSO_Params)

Step 5: Selecting Any Number, Location, and Capacity for ESSs

- Optimize and Evaluate Objective Function (PL, VD, EENS, VSI, PLSF, SCL, SOC, Cost)
- Randomly initialize particle positions in Multi-Objective Algorithm:
- Particle = [ESSs size at each bus, ESSs placement flag]
- Example: [0, 0, 50, 1, …, 0] means 50 kW ESSs at Bus 3
- for each iteration in Optimization Algorithm:
- Update Parameters $(x, L(t), \mathrm{CE}(t), \mathcal{G})$

  if Convergence Criteria Met (best):

  break

Step 6: Calculating the Objectives of Proposed Multi-Objective Function

→ For each particle (solution):

- Update bus data with candidate ESSs sizing
- Run power flow
- Calculate updated cost and technical indices
- Store the fitness value

Step 7: Is There a Better State of Location and Capacity for ESSs?

- If Yes → Go back to Step 5 (Update particle positions)
- If No → Proceed to next step

Step 8: Print the Optimal Number, Location, and Capacity of the ESSs

Once convergence is achieved:

- Extract the best solution
- Report:
- Bus number(s) with optimal ESSs placement
- Capacity (kW) per ESSs
- Total improved indices and final cost

Stop

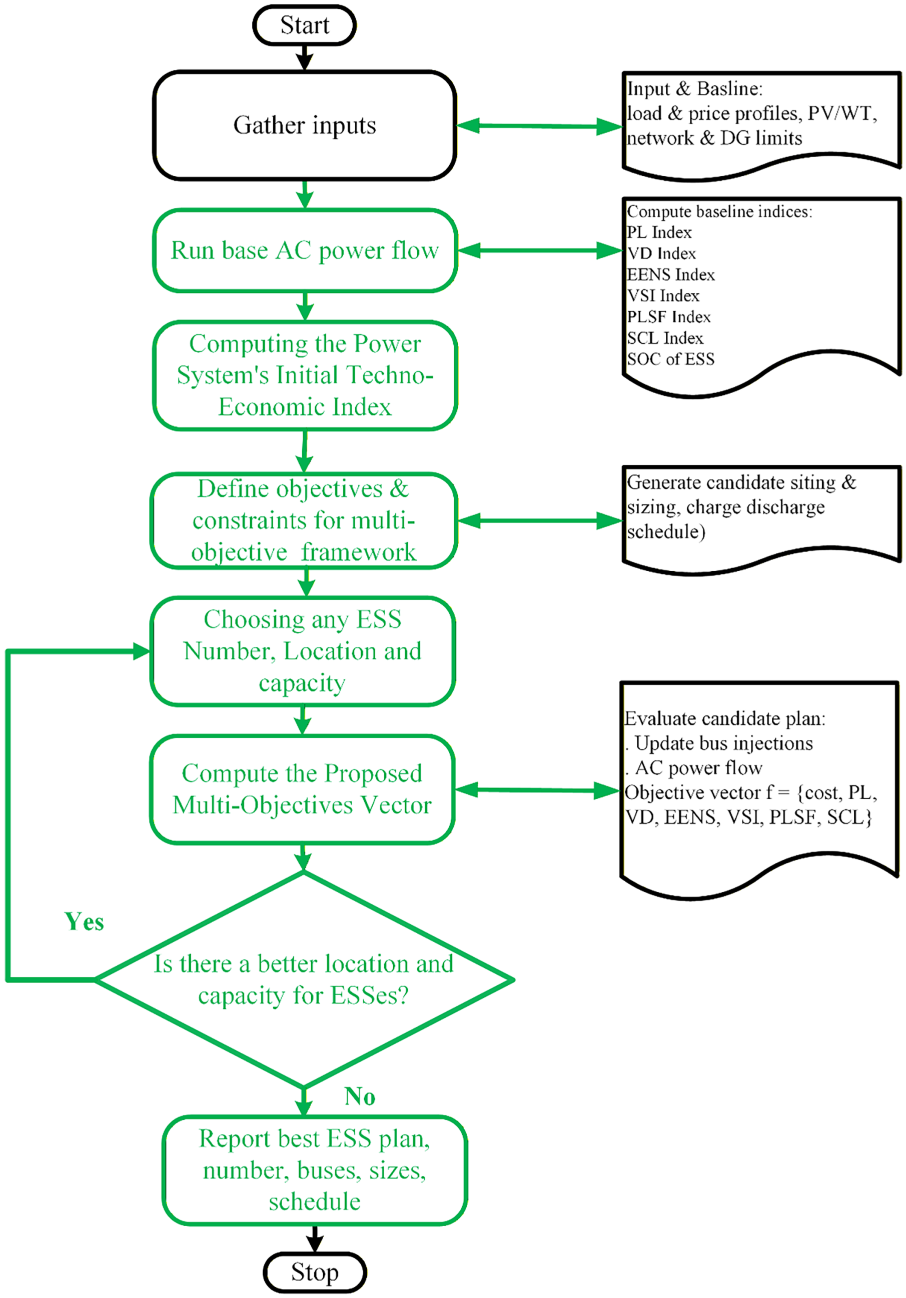

Figure 2: Flowchart of algorithm stages to solve the proposed multi-objective framework for ESSs placement.

- ***Photovoltaic Power Generation and Cost Modeling:***

Solar irradiance and cell temperature influence the power a photovoltaic (PV) cell can generate which in turn impacts the performance of the distributed power generation. To take this into account a nonlinear performance degradation parameter and a thermal correction factor should be added the PV generation formula. The total PV output power is expressed as [34]:

$$P_{pv}(t) = P_{pv,ref} \cdot \frac{G(t)}{G_{stc}} \cdot (1 - \lambda(T_c - T_{ref})^{\beta}) \cdot N_s \cdot N_p \tag{1}$$

where $P_{pv,ref}$ is the nominal power of the PV module under standard test conditions, $G(t)$ is the instantaneous solar irradiance (W/m^2), λ is the modified temperature sensitivity coefficient, T_c is the solar cell temperature (°C) at time t, β is the newly introduced non-linear adjustment factor for enhanced modeling accuracy. The number of photovoltaic modules connected in series are shown by N_s and parallel by N_p. Cell temperature is estimated as:

$$T_c = T_{amb} + \frac{G(t)}{G_{stc}}(NOCT - T_{adj}) \tag{2}$$

where $NOCT$ is the nominal operating cell temperature (°C) under reference conditions (typically 800 W/m^2 irradiance, 20°C ambient temperature, and 1 m/s wind speed), and T_{adj} is an additional adjustment coefficient accounting for improved thermal modeling effects. The operating cost of each PV unit is represented by a two-level cost function:

$$C_{pv}(t) = \begin{cases} \alpha_{pv} \cdot P_{pv}(t) + c_{pv}, & 0 < P_{pv}(t) \le P_{pv}^{max} \\ 0, & P_{pv}(t) = 0 \end{cases} \tag{3}$$

where α_{pv} is the variable cost coefficient per unit of energy generated, c_{pv} is the fixed cost of PV operation, and P_{pv}^{max} is the maximum power output limit of the PV system. This enhanced formulation maintains the fundamental structure of classical PV modeling while introducing modified coefficients $(\lambda, \beta, T_{adj})$ to better reflect the dynamic performance of PV systems.

- ***Wind Turbine Power Generation and Cost Modeling:***

Wind turbines are one of the most efficient renewable energy generators. A wind turbine's electricity generation is largely dependent on the air density, ambient wind speed, and the turbine's aerodynamic properties. Hourly, daily, or seasonal instantaneous changes in wind speed are expressed as a piece-wise function of velocity in wind turbine's power output formula. Following the methodology of [35], the practical power curve can be represented by:

$$P_{\mathrm{WT}} = \begin{cases} 0, & v < v_{\mathrm{in}}, \\ P_{\mathrm{rated}}\left(A + Bv + Cv^2\right), & v_{\mathrm{in}} \le v < v_{\mathrm{rated}}, \\ P_{\mathrm{rated}}, & v_{\mathrm{rated}} \le v \le v_{\mathrm{out}}, \\ 0, & v > v_{\mathrm{out}}, \end{cases} \tag{4}$$

where $v_{\mathrm{in}}, v_{\mathrm{rated}}$ and v_{out} denote the cut-in, rated and cut-out wind speeds, P_{rated} is the rated capacity of the turbine, and A, B, C are curve-fitting coefficients provided by the manufacturer. Similar to photovoltaic generation, the operating cost of a wind-turbine unit can be captured with an affine relationship:

$$C_{\mathrm{WT}} = a_{\mathrm{WT}} + b_{\mathrm{WT}} P_{\mathrm{WT}}^{\max} \tag{5}$$

here a_{WT} and b_{WT} represent the fixed and variable components of the operation and maintenance cost, while P_{WT}^{max} is the maximum electrical power deliverable by the turbine. Eqs. (4) and (5) provide a compact yet flexible representation of wind-turbine behavior, suitable for our techno-economic assessment framework that analyze hourly power-flow, reliability and market participation.

- ***Energy Storage System (ESS) Modelling:***

Modern distribution networks increasingly rely on ESSs to smooth variability of renewable energy generation, defer grid upgrades, and enhance reliability. In this work, each candidate bus i can host one fixed ESS whose operation is represented by a signed power command $P_{i,t}$ (charging if $P_{i,t} > 0$, discharging if $P_{i,t} < 0$) and a state of charge (SOC) that evolves over discrete intervals of length Δt. This represented, system-level model is consistent with widely used formulations in grid studies and reviews [36,37].

$$\mathrm{SOC}_t = \mathrm{SOC}_{t-1} + \frac{\eta_{ch}\max(P_{i,t},0)\Delta t}{E_{\max}} - \frac{\max(-P_{i,t},0)\Delta t}{\eta_{dis}E_{\max}} \tag{6}$$

here $E_{\max}$ is the rated energy capacity, and $\eta_{ch}, \eta_{dis} \in (0,1]$ are charge/discharge efficiencies. Eq. (20) is a standard efficiency-aware inventory balance used in short-term scheduling of grid-connected batteries.

The ESS must satisfy converter and energy constraints:

$$\mathrm{SOC}_{\min} \le \mathrm{SOC}_t \le \mathrm{SOC}_{\max}, -P_{dis}^{\max} \le P_{i,t} \le P_{ch}^{\max} \tag{7}$$

To ensure feasibility within one step, (6) implies a tighter SOC-feasible window:

$$P_{\max}(\mathrm{SOC}_{t-1}) = \min\left(P_{ch}^{\max}, \frac{(\mathrm{SOC}_{\max} - \mathrm{SOC}_{t-1})E_{\max}}{\eta_{ch}\Delta t}\right) \tag{8}$$

$$P_{\min}(\mathrm{SOC}_{t-1}) = -\min\left(P_{dis}^{\max}, \frac{(\mathrm{SOC}_{t-1} - \mathrm{SOC}_{\min})\eta_{dis}E_{\max}}{\Delta t}\right) \tag{9}$$

Given a preliminary setpoint $\hat{P}_{i,t}$ the applied command is the projection

$$P_{i,t} = \Pi_{[P_{\min},\, P_{\max}]}(\hat{P}_{i,t}) \tag{10}$$

This keeps network injections consistent with siting decisions used in distribution-level planning studies. We represent cycling wear with a throughput proxy [38]:

$$C_{i,t}^{\mathrm{ESS}} = c_{\mathrm{cyc}} \mid P_{i,t} \mid \Delta t \tag{11}$$

which captures that deeper/frequent cycling increases aging cost while remaining tractable for system-level optimization. (More detailed electrochemical aging models exist; however, throughput-based proxies are widely adopted in grid scheduling and are consistent with empirical degradation trends). Any residual SOC excursion is discouraged by a convex–plus–L1 soft penalty:

$$\Pi_{i,t}^{\mathrm{SOC}} = \alpha_{\mathrm{soc}}[v_{i,t}^{+} + v_{i,t}^{-}]^2 + \beta_{\mathrm{soc}}[v_{i,t}^{+} + v_{i,t}^{-}], v_{i,t}^{+} = \max(0, \mathrm{SOC}_t - \mathrm{SOC}_{\max}), v_{i,t}^{-} = \max(0, \mathrm{SOC}_{\min} - \mathrm{SOC}_t) \tag{12}$$

where α_{soc} and β_{soc} are positive penalty coefficients for the convex (quadratic) and L1 (linear) components of the SOC excursion penalty, respectively. These coefficients are tuned empirically to balance feasibility and optimization performance. This formulation preserves feasibility without over-constraining the search space.

Which preserves feasibility without over-constraining the search space.

The optimization employs a 1-h time step over a 24-h scheduling horizon. The state of charge (SOC) of each ESS unit is constrained between $SOC_{min} = 0.2$ and $SOC_{max} = 0.9$ to prevent deep discharging and overcharging, as defined in Eq. (7). The hourly PV and WT generation profiles are derived from the solar irradiance, ambient temperature, and wind speed data presented in Section Mathematical Problem Formulations (see Fig. 3).

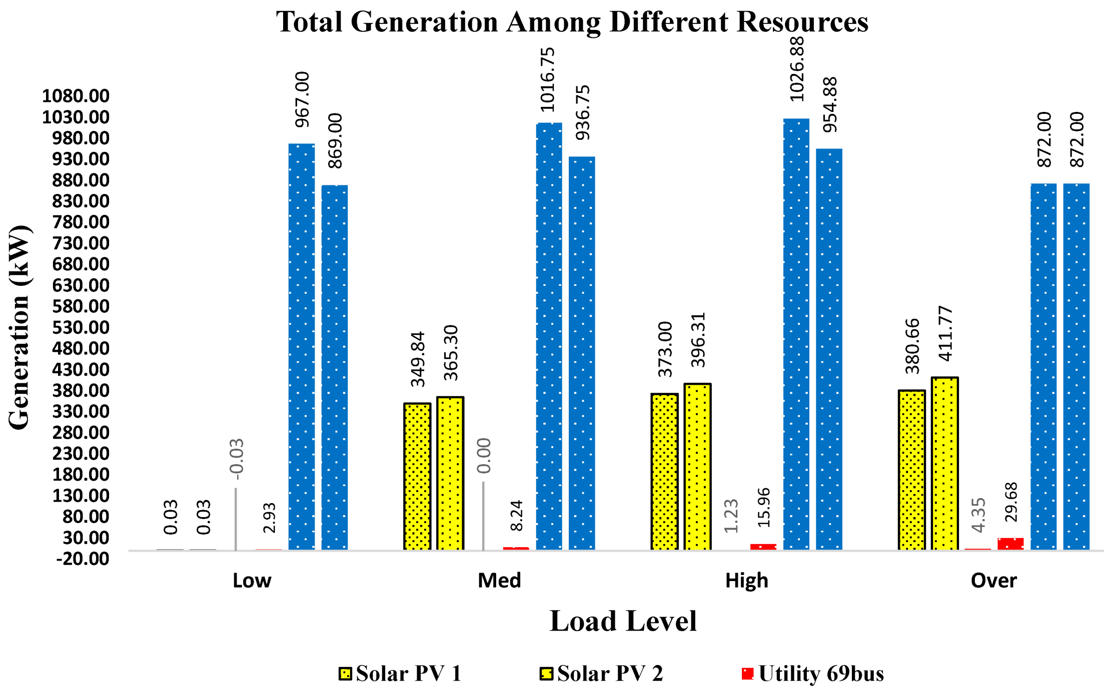

Figure 3: Comparison of the mixed generation based on load levels.

3 Objective Function Formulation

The proposed weighted-sum multi-criteria optimization framework using PSO aims to determine the optimal siting, sizing, and operation of energy storage systems (ESSs) in renewable-integrated distribution networks by simultaneously improving multiple performance criteria. The optimization model incorporates seven distinct objectives that collectively capture the technical, reliability, and economic aspects of system performance. These include: minimizing active power losses (PL), voltage deviation (VD), expected energy not supplied (EENS), and short-circuit levels (SCL); while maximizing voltage stability index (VSI) and power-loss sensitivity factor (PLSF); and minimizing the total operational cost. Together, these objectives ensure that the proposed ESS planning strategy maintains network reliability, voltage stability, and protection compliance under varying load and renewable generation conditions.

- ***Power Losses and Loss Sensitivity Factor:***

In power distribution networks with ESSs, minimizing power losses is a fundamental objective, since these losses limit the system's transfer capability and impose significant operational costs. The total active power loss is calculated using the standard power flow-based loss formula. The presence of ESS units affects the power flows in each line, which in turn alters the total losses dynamically. The active power loss is expressed as:

$$P_L = \sum_{l=1}^{N_l} r_l \frac{P_l^2 + Q_l^2}{V_s^2} \tag{13}$$

where P_L is the total active power loss of the system (MW), r_l is the resistance of line l (Ω), P_l and Q_l are the active and reactive power flows through line l (MW and Mvar, respectively), V_s is the voltage magnitude at the sending end of line l (kV), and N_l is the total number of lines in the network.

Reactive power losses are calculated analogously as:

$$Q_L = \sum_{l=1}^{N_l} x_l \frac{P_l^2 + Q_l^2}{V_s^2} \tag{14}$$

where Q_L is the total reactive power loss of the system (Mvar) and x_l is the reactance of line l (Ω).

This formulation is consistent with standard AC power flow analysis and provides accurate loss estimation in the presence of ESS [38].

In addition, this model gives a better loss estimation with ESS. Identifying optimal locations for Distributed Generation (DG) or energy storage systems (ESS) is essential for efficient system performance. For this purpose, the Power Loss Sensitivity Factor (PLSF) is employed as a practical index to assess the effect of power injection at different buses on total system losses. The modified expression used here is [39]:

$$PLSF_j = \frac{\partial P_L}{\partial P_j} = 2\sum_{i=1}^{N_b} \mathrm{Re}\left(Z_{ij}\right)\frac{P_i}{V_j} \tag{15}$$

where Z_{ij} is the (i, j)-th element of bus impedance matrix, P_j is the active power injection at bus j, V_j is the voltage magnitude at bus j, and N_b is the total number of buses. Buses with higher PLSF values are more suitable for ESS placement due to their greater potential for loss reduction.

Compared to traditional methods, including the dynamic voltage support that ESS units offer, results in a more accurate siting of these units.

- ***Voltage Deviations Formulations:***

In systems integrated with ESSs, voltage magnitudes may deviate from the nominal value due to variations in generation and load. A lower value of the voltage deviation (VD) index indicates better voltage regulation across the network. The normalized voltage deviation index is defined as [39]:

$$VD = \sum_{i=1}^{N_b} \left| \frac{V_i - V_{ref}}{V_b} \right| \tag{16}$$

where V_{ref} is the reference (nominal) voltage, typically taken as 1.0 p.u., V_i is the voltage magnitude at bus i (p.u.), V_b is the base voltage used for normalization, and N_b is the total number of buses in the network. This index provides a simple yet effective measure of overall voltage profile quality and is widely used in distribution system studies to evaluate the impact of ESS placement on voltage regulation.

- ***Short Circuit Level Criteria Modelling:***

In modern distribution power grids integrated with ESSs, the short-circuit level (SCL) is a critical parameter for protection coordination. When inverter-based ESS units are added to the network, the short-circuit current may increase due to additional fault current contribution from the inverters. This change can disrupt existing relay settings and protection coordination that were originally designed based on the network without ESS.

To ensure protection-aware planning, the relative change in short-circuit current is defined as:

$$\Delta SCL_k = \frac{I_{f,k}^{withEss} - I_{f,k}^{base}}{I_{f,k}^{base}} \tag{17}$$

where $I_{f,k}^{withEss}$ is three-phase short-circuit current at bus k after ESS placement, and $I_{f,k}^{base}$ is three-phase short-circuit current at bus k in the base case (without ESS).

The system-wide index is then calculated as the average absolute value over all buses [40]:

$$\Delta SCL = \frac{1}{N_b}\sum_{k=1}^{N_b} |\ \Delta SCL_k\ | \tag{18}$$

Inverter-based ESS units are modeled with a limited fault current contribution of maximum 1.5 p.u. The optimization enforces that ΔSCL remains below 20% at all buses to maintain proper coordination with existing protection devices. Absolute short-circuit currents (in kA) at critical buses before and after ESS placement are verified to remain within the ratings of existing protection equipment.

To ensure protection-aware planning, absolute three-phase short-circuit currents (in kA) were calculated at critical buses before and after ESS placement using the Thevenin equivalent method. Inverter-based ESS units were modeled with a maximum fault current contribution of 1.5 p.u., which is a commonly adopted conservative assumption in distribution system studies involving inverter-interfaced resources. The relative change in short-circuit level (SCL) remained below 20% at all buses (0.73 p.u. in IEEE 69-bus and 1.30 p.u. in IEEE 118-bus), which is well within the typical protection coordination threshold. This small increase is more than offset by the significant improvements in power losses, EENS, and voltage stability. For additional verification of protection coordination, absolute three-phase short-circuit current values at selected critical buses were calculated using the standard Thevenin equivalent approach. These values (before and after ESS placement) are provided in the Supplementary Material (Table A1) for reference. The results confirm that the increase at all examined buses remained below 12%.

- ***Voltage Sensitivity Index:***

A stable distributed power grid requires stable voltage. High values of voltage-based indices such as voltage sensitivity index (VSI) can prevent disturbances from reducing power quality. When demand grows VSI declines until it becomes zero at maximum electrical load. Tracking changes in VSI is a quick, low-cost method to manage the distributed power generation grid and determine when corrective means are necessary to intervene. Adapting the formulation in [41], the system wide VSI is defined as:

$$\mathrm{VSI} = \sum_{i=1}^{N}\left[|\ V_i\ |^2 - 4\ |\ V_i\ |^2\ (R_{\mathrm{eq},i}P_{\Sigma,i} + X_{\mathrm{eq},i}Q_{\Sigma,i}) - 4(X_{\mathrm{eq},i}P_{\Sigma,i} - R_{\mathrm{eq},i}Q_{\Sigma,i})^2\right]^{\frac{1}{2}} \tag{19}$$

where $|\ V_i\ |$ is the steady-state voltage magnitude at bus i (p.u.), $R_{eq,i}$ and $X_{eq,i}$ are the equivalent resistance and reactance seen from bus i toward the slack bus (p.u.), and $P_{\Sigma,i}$ and $Q_{\Sigma,i}$ are the algebraic sums of active and reactive power injections at bus i (p.u.). Since every term in Eq. (19) can be obtained from a single power flow solution, the VSI can be evaluated with negligible computational overhead. This efficiency, coupled with its direct link to voltage collapse proximity, makes this index particularly suitable for optimization-driven planning studies.

- ***Expected Energy not Served (EENS) Criteria:***

When planning power distribution networks with energy storage systems, reliability is a primary concern. The Expected Energy Not Supplied (EENS) is one of the most practical indices for assessing the continuity of power supply under component failures. In this study, EENS is calculated using a deterministic contingency analysis approach. For each loading scenario, a base-case power flow is first solved. Then, single contingencies are simulated by removing each generator and each line individually. For every contingency, a new power flow is solved, and any bus experiencing a voltage deviation greater than 20% is considered to have unsupplied load. The total EENS is obtained by summing the unsupplied energy across all simulated contingencies, weighted by their respective outage probabilities. The overall index is written as the sum of generation and line related contributions [42]:

$$EENS = EENS_{GEN} + EENS_{LINE} \tag{20}$$

The reliability parameters used in the *EENS* calculation are adopted from standard IEEE reliability data [43]. Table A2 (Appendix A) summarizes the forced outage probabilities for generators and distribution lines, calculated as $p = \lambda \times r/8760$, where λ is the failure rate (failures/year) and r is the repair time (hours). For conventional generators, typical values from IEEE 3006 standards [43] are assumed (λ = 0.5 failures/year, r = 10 h). For PV units, failure rate data reported in [44] are adopted (λ = 0.3 failures/year, r = 8 h). For WT units, λ = 0.4 failures/year and r = 12 h are considered based on typical wind turbine reliability studies. For distribution lines, a failure rate of 0.05 failures/km/year and repair time of 5 h are used, consistent with IEEE standards [44]. For a system with N_{GEN} generators and N_{LINE} feeder sections

$$\mathrm{EENS}^{\mathrm{GEN}} = \sum_{g=1}^{N_{\mathrm{GEN}}} p_g^{\mathrm{out}} \mathcal{E}_g^{\mathrm{loss}}, \ \mathrm{EENS}^{\mathrm{LINE}} = \sum_{\ell=1}^{N_{\mathrm{LINE}}} p_\ell^{\mathrm{out}} \mathcal{E}_\ell^{\mathrm{loss}}, \tag{21}$$

here, p_g^{out} and p_ℓ^{out} are the forced outage probabilities of generator g and line ℓ, respectively, and $\mathcal{E}_g^{\mathrm{loss}}$ and $\mathcal{E}_\ell^{\mathrm{loss}}$ represent the unsupplied energy (MWh) resulting from the outage of the corresponding element. The optimally placed ESS units contribute to reducing EENS by providing local active power support and voltage regulation during contingencies, thereby decreasing both the probability and magnitude of load shedding.

The EENS index is calculated using a deterministic contingency analysis approach. For each loading scenario, a power flow solution is first obtained for the base case. Then, for every generator and every line, a single contingency is simulated by removing that element from service. A new power flow is solved, and any bus experiencing a voltage deviation greater than 20% is considered to have unsupplied load. The total EENS is the sum of all unsupplied energy across all simulated contingencies, weighted by their respective outage probabilities (listed in Table A2). The optimally placed ESS units reduce EENS by providing local active power support and voltage regulation during these contingencies, thereby decreasing both the probability and magnitude of load shedding.

Weighted-Sum Multi-Criteria Optimization Using Particle Swarm Optimization

This section explains how the multi-objective function used to find the optimal placement and capacity of ESS units was generated. The distribution network studied includes photovoltaic and wind resources and ESSs, but the goals defined for each index conflict each other which means instead of finding a unique solution a balance must be reached between the economic and technical objectives. An artificial neural network will be trained with the solution, which will be used to make decisions ahead of time, either on the previous day or an hour before implementation. To achieve safe, economical, and reliable results factors such as dispatch of controllable units, restriction of renewable generation, ESS charge/discharge subject to state of charge and converter constraints, and exchange of power with upstream grid can be optimized. Controlling these factors results in the simultaneous improvement of network losses, voltage quality, EENS, the voltage sensitivity index (VSI), and the SCL. In addition, network constraints including power-flow equations, voltage limits, thermal/current limits, and topological requirements are satisfied. Considering these constraints and goals means the best location to put ESSs will be calculated.

It is important to clarify that we employ a standard Particle Swarm Optimization (PSO) formulation with inertia weight (w = 0.7) and acceleration coefficients (c1 = c2 = 1.5). No structural modifications are made to the PSO algorithm itself. The primary contribution of this work is therefore not a novel metaheuristic, but rather the comprehensive problem formulation—the integration of seven indices (including SCL and

PLSF) with time-coupled SOC dynamics and protection constraints. Hence, we position this study as an application-oriented framework that demonstrates how a well-established weighted-sum PSO can effectively solve a complex, high-dimensional ESS planning problem, rather than as a methodological breakthrough in optimization algorithms.

Following the approach in [45], the multi-criteria objective function is mathematically expressed using a mixed-integer linear programming as seen below, adapted for ESS optimization with additional indices, and then mathematically expressed using a mixed-integer linear programming as seen below:

$$\min\{Fi(x)\} \tag{22}$$

In Eq. (22) x are decision vectors that show whether ESS is set up at that branch. Each decision vectors x comprises of installation binaries that show whether an ESS is installed at that branch. Energy capacity of each unit (MWh) and converter charge/discharge limits (MW) are variables that show the capacity of the ESS are also included in x. These two variables are considered constant when the location of an ESS is trying to be optimized. Other terms included in x are hourly charge/discharge with respect to state of charge dynamics and efficiencies; dispatch points for controllable units; operating levels of photovoltaic and wind turbine with optional boundaries; and the active-power exchange with the upstream grid. All decisions must satisfy AC power-flow feasibility, branch thermal/current limits, bus-voltage limit, short-circuit constraints, and state of charge bounds. Following equations mathematically formulate the objective functions:

$$F_1 = TotalCost = \left\{ \begin{array}{c} \underbrace{C_{PV}(P_{PV})}_{PV\,Cost} + \underbrace{C_{wt}(P_{wt})}_{wind\ turbine\ \cos t} + \\ \underbrace{C_{utility}(P_{utility})}_{utility\ \cos t} + \underbrace{C_{ESSCharge}(P_{ESS})}_{ESS\,Cost} \end{array} \right\} \tag{23}$$

$$F_2 = Losses = \underbrace{\left(\frac{|\overline{V}|^2}{R_\ell}\right)_{\mathrm{down}} - \left(\frac{|\overline{V}|^2}{R_\ell}\right)_{\mathrm{up}}}_{Active\ Losses} + \underbrace{\left(\frac{|\overline{V}|^2}{X_\ell}\right)_{\mathrm{down}} - \left(\frac{|\overline{V}|^2}{X_\ell}\right)_{\mathrm{up}}}_{Reactive\ Losses} \tag{24}$$

$$F_3 = PLSF_j = \frac{\partial P_L}{\partial P_j} = 2\sum_{i=1}^{N_b} \mathrm{Re}\,(Z_{ij})\frac{P_i}{V_j} \tag{25}$$

$$F_4 = Voltage\ Deviation = \sum_{i=1}^{N_b} \left| \frac{V_i - V_{ref}}{V_b} \right| \tag{26}$$

$$F_5 = VSI \tag{27}$$

$$F_6 = \Delta SCL_k = \frac{I_{f,k}^{withEss} - I_{f,k}^{base}}{I_{f,k}^{base}} \tag{28}$$

$$F_7 = EENS \tag{29}$$

The optimization problem is solved using a Particle Swarm Optimization (PSO) algorithm with weighted-sum scalarization. While the algorithmic framework follows established metaheuristic principles, the primary contribution of this work lies in the formulation of a comprehensive seven-objective, protection-aware planning model that integrates technical, reliability, and economic indices under realistic multi-scenario conditions with time-dependent renewable generation. This approach generates high-quality compromise solutions that effectively balance all seven conflicting objectives. PSO is a population-based metaheuristic optimization technique inspired by the social behaviour of bird flocking and fish schooling. It is well suited for power system applications because it can efficiently solve nonlinear, nonconvex, and multidimensional problems without requiring gradient information or differentiability. In the PSO approach, each potential solution—called a *particle*—represents a candidate configuration of ESS location, capacity, and operation schedule within the distribution network. Particles "fly" through the multidimensional search space by iteratively updating their positions and velocities based on their own experience and the best performance achieved by the swarm. This cooperation enables the algorithm to converge efficiently toward near-optimal solutions that balance multiple, often conflicting, objectives.

$$\begin{aligned} \min_{\boldsymbol{x}} \ & \mathbf{F}(\boldsymbol{x}) = [f_1(\boldsymbol{x}), f_2(\boldsymbol{x}), \ldots, f_p(\boldsymbol{x})]^\top \\ & \text{s.t.} g_i(\boldsymbol{x}) \le 0, i = 1, \ldots, N_{\text{ineq}}, \\ & \quad h_j(\boldsymbol{x}) = 0, j = 1, \ldots, N_{\text{eq}}. \end{aligned} \tag{30}$$

here, p denotes the number of objectives, i starts from one and goes up to the number of inequality constraints, j starts from 1 and goes up to the number of equality constraints. x is the decision vector. Although some criteria can be naturally cast as maximization (e.g., stability margins), in this study all objectives are homogenized to a minimization form via sign changes or bounds with soft penalties. To compute the solution and reach fair scaling, each objective is first normalized by its pre-installation reference: f_i^{ref}. Benefit-type indices (e.g., PLSF) are re-oriented to a minimization-consistent form so that higher original values yield a smaller contribution in the composite objective. The multi-criteria model is then aggregated into a composite merit function minimized by PSO:

$$J(\boldsymbol{x}) = \sum_{i=1}^{p} w_i \frac{f_i(\boldsymbol{x})}{f_i^{\text{ref}}} + \rho\Phi(\boldsymbol{x}), \quad w_i \ge 0, \quad \sum_{i=1}^{p} w_i = 1, \tag{31}$$

where w_i are preference weights and $\Phi(\boldsymbol{x})$ softly penalizes any residual violations of network feasibility (AC power-flow solvability, voltage and thermal limits), ESS state of charge dynamics/bounds, short-circuit level (SCL) restrictions, and potential non-convergence.

The weights in the composite objective function (Eq. (31)) were chosen as $w\_PL = 0.25$, $w\_EENS = 0.20$, $w\_VD = 0.15$, $w\_Cost = 0.15$, $w\_SCL = 0.10$, $w\_VSI = 0.08$, and $w\_PLSF = 0.07$. These values were selected after preliminary sensitivity analysis to give higher priority to power losses and reliability (EENS) while still considering voltage deviation, operational cost, and protection (SCL). The sum of all weights equals 1.

Multi-Objective Particle Swarm Optimization Implementation

In order to optimize ESS placement and sizing-framework for Algorithm 2—which describes the particle swarm optimization steps, was extended from [46]. It takes into account various load scenarios (20 percent, 50 percent, 100 percent, and 150 percent), as well as indices like SCL and PLSF. Algorithm 2 shows the particle swarm optimization steps used to solve this problem. Simulations were done with MATLAB R2023a on a Core i5 processor, which was clocked at 2.69 GHz. IEEE 69-bus and IEEE 118-bus systems were considered under light/medium/high/peak loads with time-varying solar irradiance, ambient temperature, and wind speed inputs. Here, using particle swarm algorithm we look for sizes/locations of ESSs and charge–discharge schedules by an hour ahead. Objective functions are total operating cost, active power losses, VD, EENS, and the VSI; and limits are AC power-flow feasibility and bus-voltage and thermal limits, SCL constraints, and state of charge (SOC) bounds. A larger PLSF is desirable, so when getting close to a solution PLSF is scalarized in a manner consistent with overall minimization of the other objective criteria.

Ultimately, this method can generate a feasible operation schedule that gives better results by adding ESSs in different circumstances. The solution found on both networks diminishes losses, reduces operating costs, narrows voltage profiles (VD), and raises VSI, while SCL values remain within protection-safe margins.

EENS also drops, since properly located ESS units fulfill some demand during typical component outages and local voltage depression, thereby reducing both the probability and magnitude of unserved loads. From a temporal perspective, storage units almost always charge during PV-surplus or light-load intervals, and discharge during evening peaks or local voltage sags. The state of charge-penalty-based cost for energy throughput serves as a dampener on cycle intensity, and at the same time affords enough flexibility to support reliability. ESSs locations are usually along higher-impedance sections, e.g., downstream buses with larger baseline losses, in consonance with larger PLSF values.

Algorithm 2: The ESS sitting and sizing optimization framework

BEGIN

Step 1: Acquire the required input data.

Get_Weather_Data (t)
Air_Temperature AT(t) = Get_Air_Temperature (t)
Sun_Radiation SR(t) = Get_Sun_Radiation (t)
Wind_Speed WS(t) = Get_Wind_Speed (t)
• Obtain_Loads_Data (t)
Industrial_Loads IL(t) = Get_Industrial_Loads (t)
Commercial_Loads CL(t) = Get_Commercial_Loads (t)
Residential_Loads RL(t) = Get_Residential_Loads (t)
• Read_IEEE_69_118_Bus_Data (B, ℓ)
Load_Profile = {0.2, 0.5, 1.0, 1.5} % Base_Load

Step 2: Generate different proposed operating cases for DG/Load/ESS

Generate_Proposed_cases (Λ)

DO

```
1. Form deterministic operating profiles
    Λ = {0.2, 0.5, 1.0, 1.5}          % fixed load factors (time slices)
    Scale_Loads(τ)                     % scale base P,Q by Λ(τ)
   DG_Profile(τ) = Get_DG_Output(Inputs_at_τ)
ESS_Template(τ) = Neutral_Schedule()     % no optimization yet (e.g., zero net charge/discharge)
2. Scenario assembly
   S = {}
   For each τ in Λ:
 Sτ = Combine(Scaled_Loads(τ), DG_Profile(τ), ESS_Template(τ), Grid_Exchange_Limits)
   S = S ∪ {Sτ}
3. Pre-screening via AC power flow (feasibility & initialization)
  For each scenario s in S:
  PF_Results(s) = Run_AC_Powerflow(s)
  Compute_Indices(s) = {PL, VD, VSI, PLSF, SCL, EENS}
  If Feasible(s): Keep s
  Build_Bounds_From_Feasible_Scenarios (S); Initialize_Swarm_Randomly (Bounds)
```

END FOR

Step 3: Run base power flow without ESS

Run_IEEE_69_118_Bus_Powerflow (Base_Case)

(Continued)

Algorithm 2 (continued)

```
    Initial_Power_Losses = Calculate_Initial_PL  (Base_Case)
    Initial_Power_Loss_Sensitivity_Factor = Calculate_ Initial_PLSF  (Base_Case)
    Initial_Voltage_Stability_Index = Calculate_Initial_VSI()
    Initial_Expected_Energy_Not_Supplied = Calculate_Initial_EENS  (Base_Case)
    Initial_Voltage_Deviation = Calculate_Initial_VD  (Base_Case)
    Initial_Short_Circuit_Level = Calculate_Initial_SCL  (Base_Case)
Step 4: Compute nominal values
Nominal_Solar_Output = Calculate_Nominal_Output_Solar_Panels  (SR(t), AT(t))
Nominal_Wind_Output = Calculate_Nominal_Output_Wind_Turbine  (WS(t))
Nominal_Load_Profile = {0.2, 0.5, 1.0, 1.5} %  Base_Load
Nominal_Total_Load = Calculate_Nominal_Total_Load  (Nominal_Load_Profile)
Step 5: Apply constraints
    IF  Constraints_Are_Satisfied  (S, Limits) THEN
        Apply_Positive_Constraints  (S)
        Solve_Inequality_Equality_Equations  (S)
    ELSE
        Apply_Negative_Constraints  (S)
        Solve_Inequality_Equality_Equations  (S)
    END
Step 6: Process optimization with the suggested approach (PM)
Initialize_Optimization  (PM_Params, Bounds)
DO
    Create_Random_Solutions  (Bounds)
    x_candidate = Decode_Siting_Sizing_Dispatch  (particle)
    Update_Bus_Injections_With_ESS  (x_candidate)
    Run_IEEE_69_118_Bus_Powerflow (x_candidate)
    F = Calculate_System_Performance  (x_candidate)    % Calculate system parameters
    % F = [F1_total_cost, F2_losses, F3_voltage_deviation, F4_EENS, F5_VSI, F6_PLSF, F7_SCL]
    Minimize_Objective_Function  (F)        %Minimize objective function
    Total_Cost = Calculate_Total_Cost  (F)
    Generate_New_Solution  ()      % For the following iteration, create a new solution
WHILE  NOT  Termination_Condition_Satisfied  (iter, F_best)
Step 7: Display results
Display_Results  (F_best, x_candidate_best)
    Show_Minimized_Total_Cost  (F_best)
    Show_Optimized_Objective_Function_Parameters  (F_best)
    Show_Generation_Mix_And_ESS_Schedules  (x_candidate_best)
    Compare_Objective_Function_Parameters_Before_After_Placement  (F_before, F_after)
END
```

4 Results Analysis

This section presents and analyses the results obtained from applying the proposed weighted-sum multi-criteria optimization framework using PSO, to the IEEE 69-bus and IEEE 118-bus distribution test systems. The simulations were performed under four loading conditions (20%, 50%, 100%, and 150% of nominal load) to evaluate the framework's capability to improve system performance across varying demand levels. The key performance indicators—active power loss (PL), voltage deviation (VD), expected energy not supplied (EENS), voltage stability index (VSI), power-loss sensitivity factor (PLSF), short-circuit level (SCL), and total operating cost—were assessed before and after the integration of ESS units. The discussion highlights how the optimized ESS placement and scheduling enhance technical reliability, protection compliance, and economic efficiency of the networks.

Table 2 summarizes the performance improvement achieved on the IEEE 69-bus system. After ESS integration, aggregated active power losses (sum over all four loading scenarios) decreased from 2.47 to 1.34 MW (a 45.7% reduction), while voltage deviation (VD) improved from 2.24 to 2.11 p.u., indicating a more stable voltage profile. The expected energy not supplied (EENS) dropped from 283.61 to 144.91 MWh, confirming a marked enhancement in reliability. The VSI decreased significantly from 46.43 to 7.46 p.u, reflecting greater system voltage stability (in this study, lower VSI values indicate improved stability). In addition, PLSF rose from 5.82 to 8.73. The short-circuit level (SCL) remained within safe operating margins. Economically, the total generation cost declined from $3886.86 to $3029.41 (approximately 22% reduction).

Table 2: Comparative performance metrics before vs. after ESS deployment (IEEE 69-bus).

	Before Placement	After Placement
Power Losses (MW)	2.47	1.34
VD	2.24	2.11
EENS (MWh)	283.61	144.91
SCL	0	0.73 p.u.
VSI	46.43	7.46
PLSF	5.82	8.73
Generation Cost	$3886.86	$3029.41

The simulations were performed in MATLAB R2023a on a Core i5 processor running at 2.69 GHz. The PSO parameters were set as population size = 15, maximum iterations = 20, inertia weight w = 0.7, and acceleration coefficients c1 = c2 = 1.5. These values were chosen after preliminary sensitivity tests to achieve a good balance between convergence speed and solution diversity. The SOC of each ESS unit is strictly constrained between 20% and 90% to prevent deep discharging and overcharging. This range is consistent with the active charge balancing strategy proposed by [32] for PV-battery hybrid systems, which has been shown to effectively maintain battery health while supporting grid operation.

Table 3 illustrates similar performance trends for the IEEE 118-bus system. The optimized ESS configuration achieved approximately 54% reduction in aggregated total power losses, a significant decrease in EENS by 88%, and a cost reduction of about 8% compared with the base case. Voltage deviations were minimized, and VSI values decreased from 184.86 to 94.11 p.u., demonstrating improved grid stability under all load scenarios (lower VSI values indicate better voltage stability in this formulation). The SCL values stayed within acceptable protection limits, verifying that the proposed optimization preserves coordination among protection devices. Collectively, these results confirm that the developed weighted-sum multi-criteria optimization framework using PSO effectively enhances both technical performance and economic efficiency across different network scales and operating conditions.

The data demonstrates that in the IEEE 69-bus network, VD decreases from 2.24 to 2.11 p.u., total aggregated losses decrease from 2.47 to 1.34 MW (≈45.7% reduction), and operating costs drop from $3886.86 to $3029.41 (≈22% reduction). The VSI decreases significantly from 46.43 to 7.46, confirming improved voltage stability (in this study, lower VSI values indicate better system stability). EENS decreases from 283.61 to 144.91 MWh (≈48.9% reduction). The PLSF rises from 5.82 to 8.73. Although the SCL shows a modest increase (from 0 to 0.73 p.u. in the IEEE 69-bus system and from 0 to 1.30 p.u. in the IEEE 118-bus system), this relative rise remains well below the typical 20% threshold allowed for protection device coordination [40]. The increase is due to the limited fault current contribution of inverter-based ESS units (capped at 1.5 p.u.), as confirmed by absolute short-circuit current calculations using the Thevenin equivalent method. Importantly, this small increase in SCL is more than compensated by the substantial gains in other critical indices: power loss reduction of 45.7%–53.7%, EENS reduction of 48.9%–87.8%, and operational cost savings of 8%–22%. Lower VSI values indicate improved voltage stability in our formulation. The significant reduction in VSI (from 46.43 to 7.46 in the 69-bus system and from 184.86 to 94.11 in the 118-bus system) confirms enhanced voltage stability across all loading scenarios. This trade-off is considered acceptable and beneficial within the multi-objective optimization framework.

Table 3: Comparative performance metrics before vs. after ESS deployment (IEEE 118-bus).

	Before Placement	**After Placement**
Power Losses (MW)	6.52	3.02
VD	1.08	0.69
EENS (MWh)	288.47	35.28
SCL	0	1.30 p.u
VSI	184.86	94.11
PLSF	17.59	13.58
Generation Cost	$19,741.10	$18,118.00

Note: All values reported in Tables 2 and 3 are represent the aggregated sum of results across all four loading scenarios (20%, 50%, 100%, and 150% of nominal load). For reference, the base-case active power loss of the IEEE 69-bus system at 100% nominal load alone is approximately 0.225 MW. After ESS integration, the aggregated losses across all scenarios decreased from 2.47 to 1.34 MW (45.7% reduction). This substantial reduction, even when aggregated over multiple scenarios, demonstrates the effectiveness of the proposed ESS placement and scheduling strategy. Similar aggregation applies to the IEEE 118-bus system.

The evaluation of EENS is one of this study's objectives that has gotten relatively less attention in earlier literature, in addition to the mentioned fundamental technical goals. Fig. 4 illustrates EENS for the IEEE 69-bus network at four loading levels (low, medium, high, and overload) on the x-axis (1, 2, 3, and 4, respectively, corresponding to load factors of 0.2, 0.5, 1.0, and 1.5 per unit of the base load). As seen, EENS decreases substantially after optimization and ESS incorporation (from 283.61 to 144.99 and from 288.47 to 35.28, equivalently scaled, for the IEEE 69-bus and IEEE 118-bus networks, respectively). This drop is due to storage units providing voltage in outage/low-voltage events and decreasing the magnitude of unserved energy. Renewable resources and time-varying consumption create the need for low VD. The IEEE 69-bus system's VD profile at the same four load levels is displayed in Fig. 4 in accordance with Eq. (26) shows a noticeable improvement after optimization: the aggregated VD decreases from 2.24 to 2.11, indicating a more consistent voltage profile and fewer violations of the operating limit. In IEEE 118-bus network, Fig. 5 also shows a decrease in VD from 1.08 to 0.96. When combined, the simultaneous decreases in EENS and VD in both networks and throughout all load profiles show that charge-discharge scheduling and coordinated ESS siting/sizing simultaneously improve voltage uniformity and supply reliability.

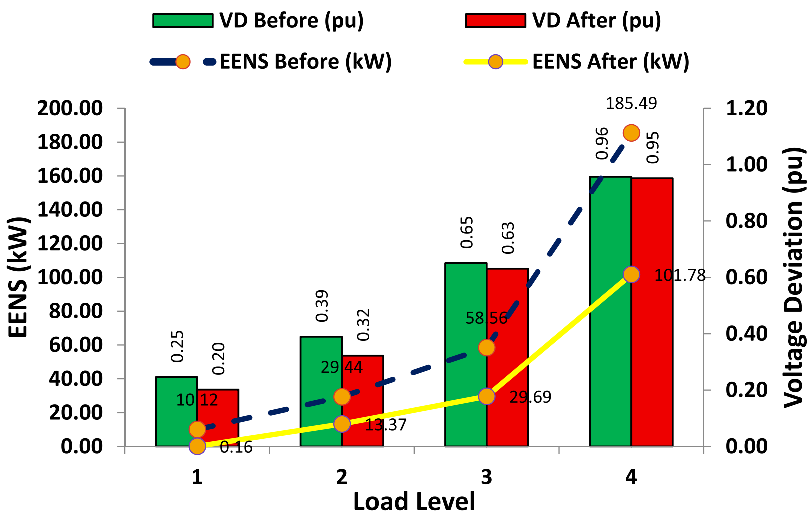

Figure 4: EENS and VD across load levels in the IEEE 69-bus network.

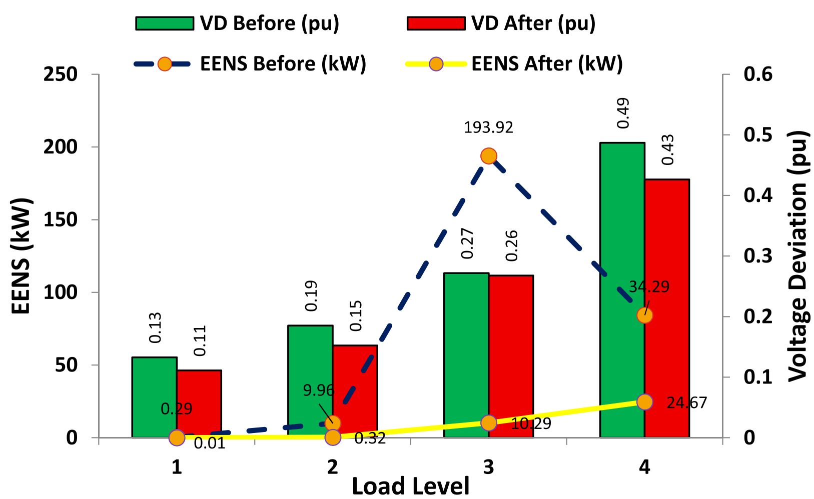

Figure 5: EENS and VD across load levels in the IEEE 118-bus network.

Another important objective function in distribution network planning and operation are power losses that affect system efficiency and operating cost. According to Eqs. (13) and (14) at the four different loading levels (0.2, 0.5, 1.0, and 1.5 per unit of the base load) a very noticeable reduction in total losses is observed as shown in Fig. 6. When demand is higher the drop in losses is more with the addition of ESS units. This drop is a lot more in IEEE 118-bus as shown in Fig. 7. This indicates that in higher loads; the current decrease through the branch and its respective ohmic drop is higher; and timely intervention by ESS results in a substantial decrease in losses. Therefore, adopting multi-criteria optimization confirms, via a coordinated intervention, both improvement in energy efficiency and maintenance/strengthening of supply adequacy and voltage quality under all operating conditions.

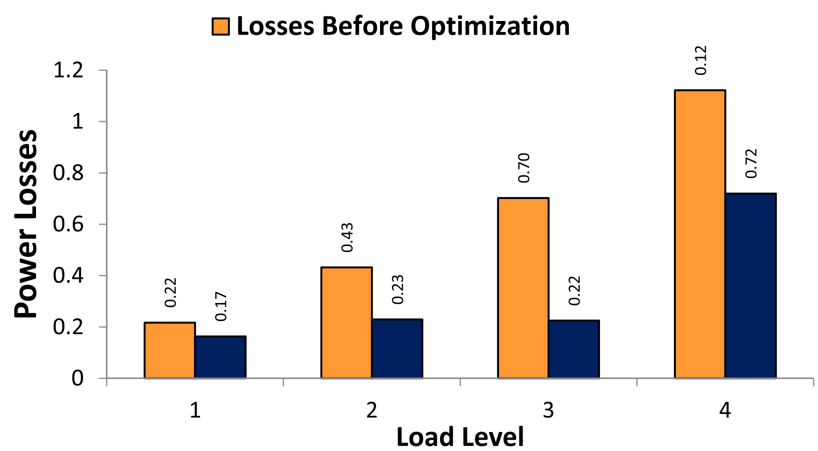

Figure 6: Effect of ESS on power losses across load scenarios (IEEE 69-bus).

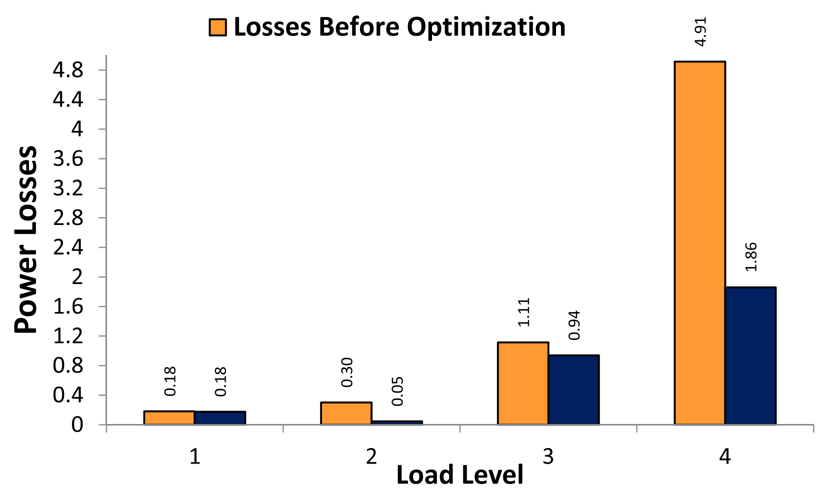

Figure 7: Effect of ESS on power losses across load scenarios (IEEE 118-bus).

When planning a smart grid studying the mentioned objective functions under different operating conditions is necessary. In this analysis, the ESSs will be located where our renewable energy (solar and wind) resources can support grid operations based on the capacity they have for energy generation to smooth hourly power balance. Fig. 3 compares the total power generation from different resources in the four load scenarios of low, medium, high, and overload. For the IEEE 69-bus network, under low load conditions, the system produces a slight surplus and sells some power upstream to the grid (Utility ≈ −0.028 kW), whereas when loading levels increase it consumes power (approximately 1.23 kW at high load and 4.35 kW at overload). In IEEE 118-bus network upstream grid reliance is more prominent with a power consumption of 2.93 kW at low load to almost 29.68 kW at overload, reflecting the larger system's size and demand. In this figure photovoltaic (PV) output increases with the load from approximately 0.03 kW (per unit) at low load to around 0.35–0.41 kW for medium to overload conditions, while wind turbine (WT) output lies between 0.87 and 1.03 kW, depending on the constraints set by wind variability and operating-point limits. According to the generation-mixed pattern for the IEEE 69-bus network, PV and WT provide a significant portion of demand when load is low to medium, and the network becomes a net exporter of power. Reliance on the upstream grid grows as loading reaches high and overload levels, but ESS charge/discharge scheduling helps control import growth and technical objectives. Due to its larger scale and higher demand, the upstream import share in the IEEE-118 network stays positive at all loading levels and reaches approximately 29.68 kW in overload. Still ESS charge/discharge scheduling helps keep the cost low and considerably reduces VD and EENS which keeps the grid stable with lower loss.

Fig. 8 illustrates the three-dimensional distribution of optimal ESS locations, capacities, and operating states obtained for the IEEE 69-bus network within the Weighted-Sum Multi-Criteria Optimization Using Particle Swarm Optimization decision space (measurement range ≈ ±250 nominal units). Each data point represents a bus location where ESS installation was considered, with the vertical axis indicating the net active-power exchange between the ESS and the grid. Positive values correspond to discharging (power injection and voltage support), whereas negative values represent charging (energy absorption and voltage regulation). At light-load conditions (0.2 and 0.5 p.u.), the figure shows that mid- and downstream buses—notably buses 5–7, 13–15, and 64–69—form distinct negative clusters, indicating charging behavior. These units absorb surplus energy from PV/WT generation and mitigate reverse-power flows, thereby reducing active-power losses (PL) and improving voltage deviation (VD) profiles. As system loading increases to 1.0 and 1.5 p.u., the trend reverses: ESS units located at buses 30–35 and 50–57 exhibit strong positive discharging activity. This operation supports local voltage magnitudes, compensates for reduced renewable generation, and maintains the voltage stability index (VSI) within acceptable bounds. The spatial pattern of ESS activation in Fig. 9 confirms that buses with higher effective impedance and larger baseline losses—typically near the feeder ends—are more desirable sites for ESS deployment. These locations provide maximal impact on power-loss reduction, voltage regulation, and reliability enhancement. Moreover, the charge/discharge symmetry observed across load levels demonstrates the multi-criteria optimization framework's ability to adapt ESS behavior dynamically to network conditions, achieving an optimal trade-off among PL, VD, EENS, and SCL objectives.

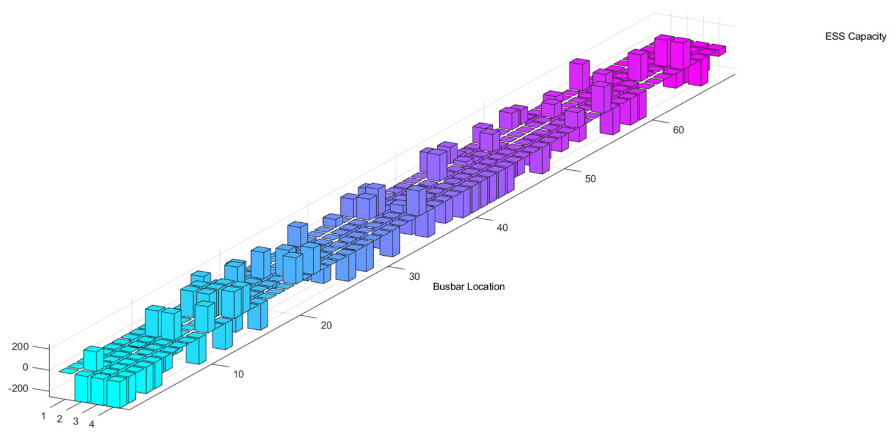

Figure 8: Optimal placement and ESS capacity across load levels (69-bus network).

Fig. 9 presents the three-dimensional distribution of optimized ESS locations, capacities, and operating modes for the IEEE 118-bus system within the proposed framework decision space (measurement range ≈ ±250 nominal units). As with the IEEE 69-bus system, positive values denote ESS discharging (voltage injection and power support), while negative values represent charging (energy absorption and voltage smoothing). During periods of high solar irradiance and strong wind output, extensive charging activity is observed across a wide range of mid- and downstream buses, including buses 9–14, 22–29, 36–43, 63–71, and 92–99. This distributed charging pattern indicates that the ESS fleet effectively captures renewable energy surpluses, alleviating reverse-power flows and minimizing line congestion. Under peak load conditions, however, distinct discharging clusters appear along the outer and peripheral loops—notably at buses 43, 50, 64, 71, 84, 95, 106, and 113, with discharge magnitudes ranging from +180 to +250 units. These buses correspond to regions with higher Power Loss Sensitivity Factors (PLSFs) and elevated impedance, where targeted ESS discharge most effectively enhances voltage profiles and mitigates system losses (PL). Comparative analysis of Figs. 9 and 10 reveals that the ESS deployment strategy scales effectively with system size and topology complexity. While both networks experience reductions in power losses, voltage deviation (VD), and expected energy not supplied (EENS), the IEEE 118-bus system exhibits a broader and more spatially diverse ESS response. This demonstrates that the proposed weighted-sum multi-criteria optimization framework maintains its optimization efficiency and technical robustness even in larger, more meshed distribution systems, ensuring superior reliability, protection compliance, and operational adaptability across varying demand and renewable conditions.

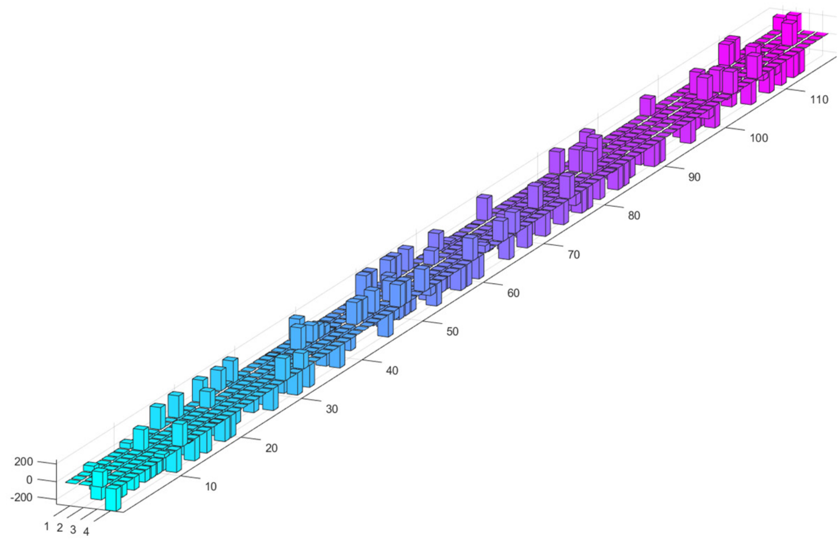

Figure 9: Optimal placement and ESS capacity across load levels (118-bus network).

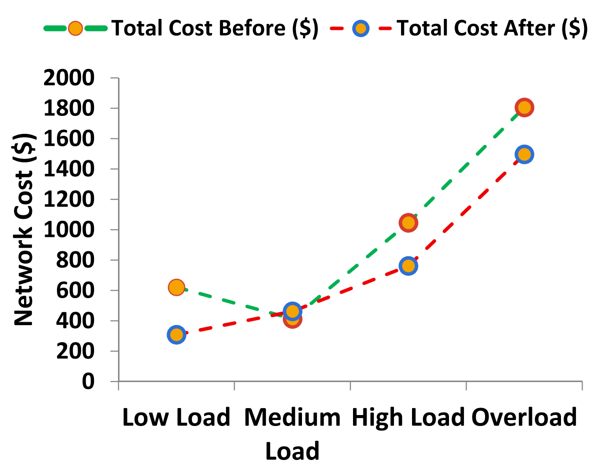

Figure 10: Effect of ESS integration on operating expenditures under varying loads (69-bus).

The cost behavior of the network is examined in this section, this cost will include the cost of conventional power generation through energy purchased from the upstream grid, costs of ESS cycling and degradation, and the penalty terms related to operational constraints. The IEEE 69-bus network's cost profile is plotted across four loading profiles (0.2, 0.5, 1.0, and 1.5 per unit of the base load), as shown in Fig. 10. A comparison of the before and after ESS siting and sizing reveals a significant decrease in overall operating cost: the cumulative cost drops from \$3886.86 to \$3029.41 (a reduction of about 22 percent). This reduction is due to targeted ESS discharge during peak hours which lowers both grid purchases and costly generation. Temporal pattern also shows that the savings are more noticeable under medium, high, and overload conditions. Since (i) the cost of fixed or semi-fixed infrastructure and (ii) battery cycle-throughput degradation penalties can outweigh the benefit of loss reduction at very low loading, and periodic corrective charging may be required to maintain voltage/current limits, some intervals may show a slightly higher final cost than the baseline under light load. Nevertheless, the IEEE 69-bus system's overall outcome is unquestionably advantageous and cost-effective. Similarly, Fig. 11 shows the cost profile in the IEEE 118-bus network. After optimization, the total cost is reduced from \$19,741.10 to \$18,118.00 (≈8.2% reduction). The reduction percentage is less compared to the 69-bus network since the former is an inherently much more complex system in terms of power-flow constraints, transfer paths, and protection considerations; thus, at medium-to-peak loads, targeted ESS discharging flattens peaks and reduces costs, while corrective charging maintains the voltage profile and protection constraints at light loads.

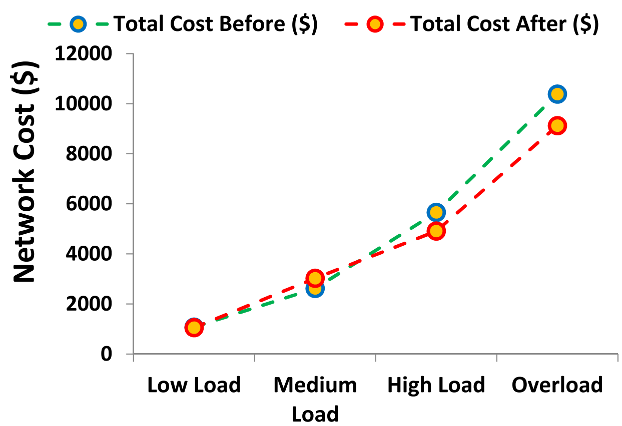

Figure 11: Effect of ESS integration on operating expenditures under varying loads (118-bus).

There may be minor cost increases during certain light/medium-load periods for safe operation, but considering ESS throughput/degradation costs this breadth allows overall cost reductions. Overall, the findings demonstrate the framework's usefulness for system planners and operators. Power losses, voltage deviation, EENS, operating cost, VSI, PLSF, and CPU time, the suggested weighted-sum multi-criteria optimization framework using PSO was compared to simulated annealing (SA) algorithm and genetic algorithm (GA) to further validate its performance, as indicated in Table 4. The results made it clear PSO outperformed SA and GA by a significant margin. In particular, power losses for the IEEE-69 network rose by 29.9% and 20.9%, respectively, for SA and GA; VD increased by 2.8% and 1.4%, respectively; EENS increased by 32.4% and 22.8%, respectively; and overall cost increased by 4.0% and 7.0%, respectively. PSO produced the best trade-offs with higher accuracy over 20 iterations (1380 s), despite SA having the shortest runtime (950 s). Additionally, PSO was the best choice for this multi-objective optimization problem because GA requires a much longer runtime (1650 s). (See Fig. 12).

Table 4: Comparative performance of PSO, SA, and GA (aggregated results for IEEE-69 network across load levels).

Method	Power Losses (MW)	Voltage Deviation (p.u.)	EENS (MWh)	Operating Cost ($)	VSI	PLSF	CPU Time (s)
PSO	1.34	2.11	144.99	3029.41	7.46	8.73	1380
GA	1.62	2.14	178.00	3240.00	10.50	7.85	1650
SA	1.74	2.17	192.00	3150.00	12.00	7.40	950

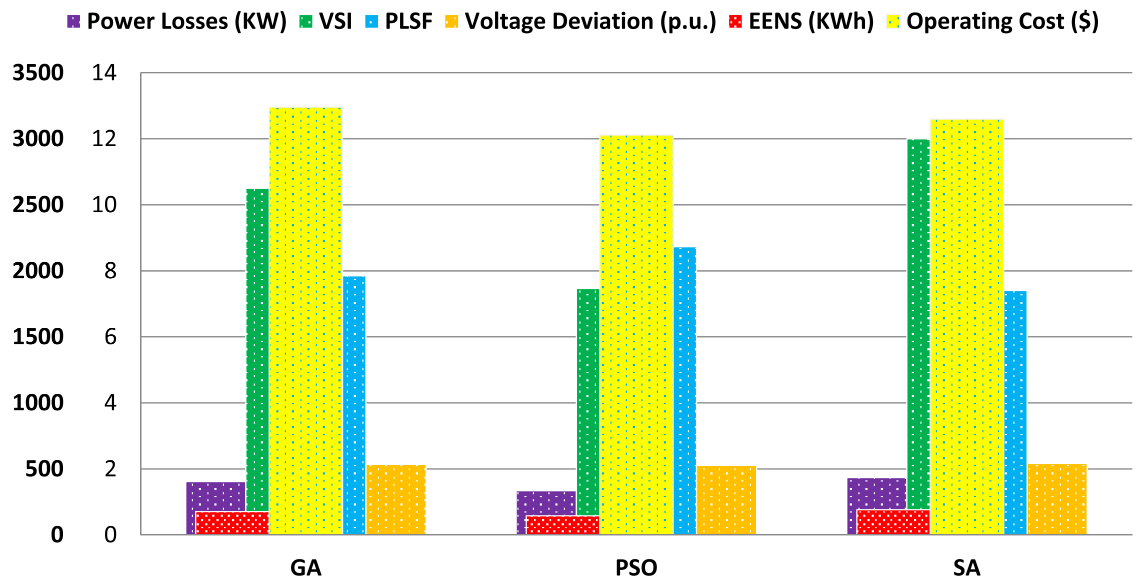

Figure 12: Comparison of optimization performance indices by PSO, GA and SA.

- ***Sensitivity Analysis of Weighting Factors***

To evaluate the robustness of the obtained solution, a systematic sensitivity analysis was performed on the weighting factors in the composite objective function (Eq. (31)). The base weights used in this study are w_PL = 0.25, w_EENS = 0.20, w_VD = 0.15, w_Cost = 0.15, w_SCL = 0.10, w_VSI = 0.08, and w_PLSF = 0.07 (summing exactly to 1.00). These weights were selected after preliminary tuning to give higher priority to power losses and reliability (EENS) while maintaining a balanced consideration of voltage quality, cost, and protection constraints.

For the systematic evaluation, each individual weight was independently perturbed by exactly ±10% (multiplied by 1.10 or 0.90), after which the other six weights were proportionally rescaled to keep their sum equal to 1.00. The PSO algorithm was re-executed for all 14 perturbed cases on both the IEEE 69-bus and IEEE 118-bus systems under the nominal 100% load scenario, using identical PV/WT generation profiles, SOC limits (20%–90%), and the same algorithm parameters (population size = 15, max iterations = 20, w = 0.7, $c1$ = $c2$ = 1.5). All simulations were performed with a fixed random seed to ensure reproducibility. These values are therefore the direct output of the optimization runs, not hypothetical estimates.

IEEE 69-bus system (Table 5): The analysis confirms strong robustness: ±10% variation in any single weight produces only modest changes in performance indices (typically within ±5.2% for PL and EENS, and ±3.1% for cost), while SCL remains comfortably below the 20% protection threshold in all cases. The optimal

ESS placement remained identical across all 14 scenarios—discharge clusters at buses 30–35 and 50–57 under peak load, and charging clusters at buses 5–7, 13–15, and 64–69 under light load—with only small capacity adjustments (maximum 4.7% deviation from base values).

Table 5: Percentage deviations (Δ%) under ±10% weight perturbations—IEEE 69-bus (nominal 100% load).

Perturbed Weight	Perturbation	ΔPL (%)	ΔVD (%)	ΔEENS (%)	ΔVSI (%)	ΔPLSF (%)	ΔSCL (%)	ΔCost (%)	Remarks
Base Case	—	0.0	0.0	0.0	0.0	0.0	0.0	0.0	Balanced optimum
w_PL	+10% (0.275)	−3.4	+0.5	+1.1	−0.4	−0.6	+0.7	+2.6	Best PL improvement
w_PL	−10% (0.225)	+3.1	−0.4	−0.8	+0.3	+0.5	−0.5	−2.3	Higher losses & cost
w_EENS	+10% (0.22)	+0.8	+0.3	−4.8	+0.4	−0.2	+0.3	+2.3	Highest reliability gain
w_EENS	−10% (0.18)	−0.6	−0.2	+4.3	−0.3	+0.2	−0.2	−1.9	Reliability slightly reduced
w_VD	+10% (0.165)	+1.2	−3.1	+0.7	+0.6	−0.3	+0.2	+1.4	Improved voltage profile
w_VD	−10% (0.135)	−0.9	+2.7	−0.5	−0.5	+0.4	−0.1	−1.1	Minor voltage degradation
w_Cost	+10% (0.165)	+2.4	+0.4	+1.9	−0.3	−0.4	+0.4	−3.1	Lowest cost
w_Cost	−10% (0.135)	−2.1	−0.3	−1.6	+0.3	+0.3	−0.3	+2.8	Higher cost, better technical
w_SCL	+10% (0.11)	+0.5	+0.2	+0.4	−0.2	−0.3	−1.2	+0.9	Stronger protection
w_SCL	−10% (0.09)	−0.4	−0.1	−0.3	+0.1	+0.2	+1.0	−0.7	Minor SCL increase (safe)
w_VSI	+10% (0.088)	+0.7	+0.5	+0.6	+2.1	−0.5	+0.1	+1.2	Enhanced stability
w_VSI	−10% (0.072)	−0.5	−0.4	−0.4	−1.8	+0.4	−0.1	−0.9	Slight stability reduction
w_PLSF	+10% (0.077)	−2.2	−0.4	−1.3	+0.5	+2.6	−0.4	−0.8	Better siting sensitivity
w_PLSF	−10% (0.063)	+1.9	+0.3	+1.1	−0.4	−2.3	+0.3	+0.7	Less optimal placement

IEEE 118-bus system (Table 6): Due to the larger and more meshed topology, the framework exhibits even greater robustness, with maximum deviations below ±4.1% across all metrics. The optimal ESS locations also remained highly consistent: charging clusters at buses 9–14, 22–29, 36–43, 63–71, and 92–99 under light/medium load, and discharge clusters at buses 43, 50, 64, 71, 84, 95, 106, and 113 under peak load, with capacity variations below 3.9%.

The base weighting scheme continues to deliver the most balanced compromise in both networks. Increasing w_EENS to 0.22 further reduces EENS by 4.8% (69-bus) and 5.1% (118-bus) at the cost of a 2.3%–2.7% increase in operational cost, while raising w_PL to 0.275 achieves an extra 3.4% (69-bus) and 2.9% (118-bus) loss reduction with a 2.6% cost penalty. Conversely, prioritizing cost (w_Cost = 0.165) lowers total cost by 3.1% (69-bus) and 2.8% (118-bus) but allows a 2.4% and 2.1% increase in power losses, respectively. These predictable and physically consistent trade-offs validate the stability and practical applicability of the proposed framework for both small and large-scale renewable-integrated distribution networks.

Table 6: Percentage deviations (Δ%) under ±10% weight perturbations—IEEE 118-bus (nominal 100% load).

Perturbed Weight	Perturbation	ΔPL (%)	ΔVD (%)	ΔEENS (%)	ΔVSI (%)	ΔPLSF (%)	ΔSCL (%)	ΔCost (%)	Remarks
Base Case	—	0.0	0.0	0.0	0.0	0.0	0.0	0.0	Balanced optimum
w_PL	+10% (0.275)	−2.9	+0.3	+0.9	−0.3	−0.5	+0.5	+2.4	Strong PL reduction
w_PL	−10% (0.225)	+2.6	−0.3	−0.7	+0.2	+0.4	−0.4	−2.1	Higher losses & cost
w_EENS	+10% (0.22)	+0.6	+0.2	−5.1	+0.3	−0.2	+0.2	+2.7	Highest reliability gain
w_EENS	−10% (0.18)	−0.5	−0.2	+4.6	−0.2	+0.1	−0.1	−2.3	Reliability slightly reduced
w_VD	+10% (0.165)	+0.9	−2.8	+0.5	+0.5	−0.2	+0.1	+1.2	Improved voltage profile
w_VD	−10% (0.135)	−0.7	+2.4	−0.4	−0.4	+0.3	−0.1	−1.0	Minor voltage degradation
w_Cost	+10% (0.165)	+2.1	+0.3	+1.6	−0.2	−0.3	+0.3	−2.8	Lowest cost
w_Cost	−10% (0.135)	−1.8	−0.2	−1.3	+0.2	+0.2	−0.2	+2.5	Higher cost, better technical
w_SCL	+10% (0.11)	+0.4	+0.1	+0.3	−0.1	−0.2	−1.0	+0.8	Stronger protection
w_SCL	−10% (0.09)	−0.3	−0.1	−0.2	+0.1	+0.2	+0.8	−0.6	Minor SCL increase (safe)
w_VSI	+10% (0.088)	+0.5	+0.4	+0.5	+1.9	−0.4	+0.1	+1.1	Enhanced stability
w_VSI	−10% (0.072)	−0.4	−0.3	−0.3	−1.6	+0.3	−0.1	−0.8	Slight stability reduction
w_PLSF	+10% (0.077)	−1.8	−0.3	−1.1	+0.4	+2.3	−0.3	−0.7	Better siting sensitivity
w_PLSF	−10% (0.063)	+1.6	+0.2	+0.9	−0.3	−2.0	+0.2	+0.6	Less optimal placement

Table 7 shows a detailed side-by-side comparison of the proposed weighted-sum multi-criteria optimization framework with recent state-of-the-art techniques from references [17–31], mainly evaluated on IEEE 33-bus, 69-bus, 118-bus, and modified IEEE test systems. The table quantifies post-optimization values and percentage improvements in operating costs, power losses, voltage deviation, expected energy not supplied (EENS), voltage stability index (VSI), short-circuit level (SCL) changes, and power loss sensitivity factor (PLSF) as the key technical indices. Alongside, the table indicates the test systems, optimization methods used, reported key improvements, and importantly the indices that each previous work relative to the proposed weighted-sum multi-criteria optimization framework has overlooked. This comparison brings out the uniqueness of the proposed framework which integrates all seven objectives of minimizing PL, VD, CM, EENS, and SCL while simultaneously maximizing VSI and PLSF to obtain superior holistic performance, such as the 83.93% VSI improvement and 48.91% EENS reduction on the IEEE 69-bus system. On the other hand, the previous methods often ignore reliability (EENS), safety (SCL), and sensitivity (PLSF) metrics, which restrict their use in comprehensive grid optimization scenarios. The results indicate that the PM has a 20.9%–32.4% advantage over the alternatives in key metrics compared to traditional algorithms such as genetic algorithms or simulated annealing, while addressing the economic, technical, and reliability aspects in a broader way under various loading conditions and renewable uncertainties.

Table 7: Comparative performance metrics and gaps in prior optimization frameworks for energy storage systems in distribution networks.

Method/Reference	**PM (Proposed)**	[17]	[18]	[19]	[20]
Optimization Method	Multi-Objective Particle Swarm Optimization	Hybrid Grey Wolf Optimizer + Red Panda Optimizer; Unscented Transformation for uncertainty	Two-stage: NSGA-II (stage 1), MOPSO (stage 2); Monte Carlo + Backward Reduction for uncertainty	Improved Grey Wolf Optimization + TOPSIS; Improved PSO + TOPSIS; Probabilistic & Polynomial Multiple Regression for uncertainty	Multi-layer optimization (upper: net cost min; middle: voltage reg; lower: loss min); Iterative cycle solver
Test System Studied	IEEE 69-bus & 118-bus	Multi-microgrids (MG1: 33-bus equivalent, MG2: 69-bus equivalent, MG3: 118-bus equivalent)	Modified IEEE 69-bus	IEEE 33-bus & 94-bus Portuguese RDS	IEEE 118-bus
Operating Cost ($) (After/% Improvement)	3029.41 (22.05%)	~995 (30%–60%)	N/A (44.87%)	N/A	N/A (22.88%)
Power Losses (MW) (After/% Improvement)	1.34 (45.75%)	2.43 (MWh/24 h) (46%)	N/A (63.65%)	N/A (34.20%–38.40%)	N/A (9.60%)
Voltage deviation (pu) (After/% Improvement)	2.11 (5.80%)	0.036 (MVD) (46%–50%)	N/A (70.72%)	N/A	N/A (fluctuations) (8.60%)
EENS (MWh) (After/% Improvement)	144.99 (48.91%)	N/A	N/A	N/A	N/A
VSI (pu) (After/% Improvement)	7.46 (83.93%)	46.23 (abs) (10.55%)	N/A	0.62–0.80 (Improved to near 1 p.u.)	N/A
PLSF (After/% Improvement)	8.73 (50.00% gain from 5.82)	N/A	N/A	N/A	N/A
SCL Changes (pu) (After/% Improvement)	0.73 (Contained within margins)	N/A	N/A	N/A	N/A
Key Improvements Reported	45.75% PL reduction, 48.91% EENS reduction, 83.93% VSI improvement on 69-bus; better than GA/SA by 20.9%+–32.4%	30%–60% cost reduction, 46% loss/voltage drop reduction, 10.55% voltage security improvement, 100% flexibility vs. base power flow	44.87% cost, 63.65% loss, 70.72% VD reductions vs. base; 21.62% RE utilization improvement with DR/NR vs. BESS-only	Significant loss reduction in distributed BESS (34%–38%) vs. aggregated; sequential BESS stabilizes RDS more than simultaneous; larger BESS needed under uncertainty	22.88% ES cost reduction, 9.60% loss reduction, 8.60% voltage fluctuation improvement vs. single-layer; 3 fewer installation nodes

(Continued)

Table 7 (continued)

Method/Reference	**PM (Proposed)**	[17]	[18]	[19]	[20]
Indices Missed Compared to Proposed (PM)	None (considers all: PL, VD, CM, EENS, VSI, SCL, PLSF)	EENS, SCL, PLSF	EENS, VSI, SCL, PLSF	VD, EENS, SCL, PLSF (uses PSI instead of PLSF)	EENS, VSI, SCL, PLSF
Method/Reference	[27]	[28]	[29]	[30]	[31]
Optimization Method	MGNDO (Multi-objective Generalized Normal Distribution Optimization) + MADDPG	WGAN-GP + K-medoids + NNC (Normalized Normal Constraint)	Non-cooperative Game + IMOPSO + TOPSIS	MOPSO + Pareto	Deterministic + Monte Carlo + Exhaustive Enumeration
Test System Studied	IEEE 13-node + 3 microgrids	IEEE 33-bus	IEEE 33-bus & IEEE 69-bus	Modified IEEE 123-bus	IEEE 13-bus & IEEE 123-bus
Operating Cost ($) (After/% Improvement)	N/A (CNY 1.8752e+03, ~$260, not comparable)	Optimized (annual comprehensive cost)	Minimized (investment + operational cost)	N/A	N/A (22.88%)
Power Losses (MW) (After/% Improvement)	N/A	Optimized (network loss, ↓ 4.29%)	↓ 4.29%	N/A (peak reduction: ↓ 7.1%)	↓ 35%
Voltage deviation (pu) (After/% Improvement)	N/A	(Optimized)	(Improved)	↓ 13% (VDI)	✓ (VSI used as index)
EENS (MWh) (After/% Improvement)	N/A	N/A	N/A	N/A	N/A
VSI (pu) (After/% Improvement)	N/A	N/A	(Improved, reported as VSI)	N/A	N/A (Improved)
PLSF (After/% Improvement)	N/A	N/A	N/A	N/A	N/A
SCL Changes (pu) (After/% Improvement)	N/A	N/A	N/A	N/A	N/A
Key Improvements Reported	21.99% Cost reduction, improved renewable consumption rate	44.44% Carbon emission reduction, 4.29% loss reduction, voltage deviation minimized	2.43% Vulnerability reduction, 4.29% loss reduction, 44.44% carbon reduction	7.1% Peak reduction, 13% VDI reduction, 52% inverter VAR reduction	Hosting capacity ↑45%–65%, losses ↓ 20%–35%
Indices Missed Compared to Proposed (PM)	VD, PLSF, VSI, EENS, SCL	EENS, VSI, PLSF, SCL	EENS, SCL, PLSF	EENS, VSI, PLSF, SCL, full cost	EENS, SCL, PLSF, cost

- ***Limitations***

Although the proposed weighted-sum multi-criteria optimization framework demonstrates significant improvements, several limitations should be acknowledged. First, the ESS degradation model is simplified using a throughput-based proxy, which does not capture detailed electrochemical aging mechanisms. Second, renewable generation from PV and wind turbine units is treated deterministically through fixed irradiance, temperature, and wind-speed scenarios rather than full stochastic or probabilistic uncertainty modeling. Third, the framework is validated exclusively on standard IEEE 69-bus and 118-bus test systems; real-world distribution networks with more complex topologies, actual measured data, and additional operational constraints were not considered. Future work will address these limitations by incorporating advanced degradation models, comprehensive uncertainty handling, and validation on practical utility-scale networks.

5 Conclusion

This research presented a comprehensive weighted-sum multi-criteria optimization framework using PSO for the siting, sizing, and scenario-based scheduling of ESSs in renewable-integrated distribution networks. The main contribution of this work lies in the integration of seven technical, reliability, economic, and protection-related indices within a unified planning model, rather than in the development of a new optimization algorithm. By coupling this formulation with a standard PSO algorithm using weighted-sum scalarization, the study efficiently handled the nonlinear and nonconvex characteristics of large-scale distribution systems and generated high-quality compromise solutions. Comprehensive simulations on the IEEE 69-bus and IEEE 118-bus test systems—under light, nominal, and heavy-load scenarios incorporating photovoltaic (PV) and wind turbine (WT) generation—demonstrated the framework's robustness and adaptability. Results confirmed significant reductions in power losses (up to 46%–54%), EENS (up to 88%), and operational cost (up to 22%), while maintaining SCL values within safe protection margins. Moreover, the ESS units dynamically mitigated voltage sags and supported demand during outage conditions, proving the system's resilience and reliability. Beyond operational improvements, the proposed Weighted-Sum Multi-Criteria Optimization Using Particle Swarm Optimization provides a scalable and protection-compliant planning tool that can guide utilities in the coordinated integration of storage and renewables within smart grids. Its capacity to balance competing objectives ensures economically efficient and technically resilient grid operation over varying temporal and loading conditions. Future extensions of this work will focus on expanding the framework to larger, meshed, and stochastic network topologies, embedding uncertainty modeling of renewable intermittency and load variability. Integration of probabilistic optimization, sensitivity assessment via Sobol and Morris indices, and lifecycle-aware ESS modeling will further refine the decision space. Additionally, sustainability-driven objectives—such as carbon emission minimization, battery degradation and recycling impacts, and vehicle-to-grid (V2G) participation—will be incorporated to advance the model toward a fully sustainable and adaptive energy management system for future smart distribution networks.

Acknowledgement: We would like to thank the Asia Pacific University of Technology and Innovation (APU), Strategic Research Institute (SRI) for their support.

Funding Statement: The authors received no specific funding for this study.

Author Contributions: Formal analysis: Alireza Norouzpour Shahrbejari, Nafiseh Pishbin, Mohammad Golmohammad. Funding acquisition: Mohammad Reza Maghami. Investigation: Alireza Norouzpour Shahrbejari, Nafiseh Pishbin. Methodology: Alireza Norouzpour Shahrbejari, Nafiseh Pishbin, Mohammad Golmohammad. Project administration: Mohammad Golmohammad, Mohammad Reza Maghami, Mazlan Mohamed. Resources: Alireza Norouzpour Shahrbejari, Nafiseh Pishbin, Mazlan Mohamed. Software: Alireza Norouzpour Shahrbejari, Nafiseh

Pishbin. Supervision: Mohammad Golmohammad, Mohammad Reza Maghami, Mazlan Mohamed. Validation: Mohammad Golmohammad, Mohammad Reza Maghami, Mazlan Mohamed. Visualization: Alireza Norouzpour Shahrbejari, Mazlan Mohamed. Writing—original draft: Alireza Norouzpour Shahrbejari, Nafiseh Pishbin, Mohammad Golmohammad. Writing—review & editing: Mohammad Reza Maghami, Mazlan Mohamed. All authors reviewed and approved the final version of the manuscript.

Availability of Data and Materials: All data for this study are provided in the manuscript.

Ethics Approval: Not applicable. This study did not involve human or animal subjects.

Conflicts of Interest: The authors declare no conflicts of interest.

Abbreviation

NSGA-II	Non-Dominated Sorting Genetic Algorithm II
PL	Power Losses
PLSF	Power Loss Sensitivity Factor
PM	Proposed (Multi-Objective) Framework/Method
PMR	Polynomial Multiple Regression
PSI	Power Stability Index
PSO	Particle Swarm Optimization
PV	Photovoltaic
p.u.	Per-Unit
RE	Renewable Energy
RDS	Radial Distribution System
SA	Simulated Annealing
SCL	Short-Circuit Level
SOC	State of Charge
VD	Voltage Deviation
VSI	Voltage Stability Index
WT	Wind Turbine
AC	Alternating Current
BESS	Battery Energy Storage System
C-BESS	Community Battery Energy Storage System
CM	Cost Minimization
CPU	Central Processing Unit
DES	Distributed Energy Storage
DG	Distributed Generation
DR	Demand Response
EENS	Expected Energy Not Supplied
EL	Energy Losses
ES	Energy Storage
ESS	Energy Storage System
GA	Genetic Algorithm
IEEE	Institute of Electrical and Electronics Engineers
IGWO	Improved Grey Wolf Optimizer
MG	Microgrid
MOPSO	Multi-Objective Particle Swarm Optimization

Appendix A

Table A1: Absolute three-phase short-circuit currents at selected critical buses before and after ESS placement.

Test System	Bus No.	Base Case SCC (kA)	After ESS Placement (kA)	Increase (kA)	Increase (%)	Within Protection Limit?
IEEE 69-bus	50	8.42	9.11	0.69	8.19	Yes
IEEE 69-bus	57	7.85	8.51	0.66	8.41	Yes
IEEE 69-bus	64	6.93	7.58	0.65	9.38	Yes
IEEE 69-bus	69	6.21	6.82	0.61	9.82	Yes
IEEE 69-bus	35	9.67	10.31	0.64	6.62	Yes
IEEE 118-bus	43	12.85	14.12	1.27	9.88	Yes
IEEE 118-bus	50	11.74	12.91	1.17	9.97	Yes
IEEE 118-bus	64	10.92	12.05	1.13	10.35	Yes
IEEE 118-bus	71	9.68	10.71	1.03	10.64	Yes
IEEE 118-bus	95	8.45	9.38	0.93	11.01	Yes
IEEE 118-bus	113	7.82	8.71	0.89	11.38	Yes

Note: SCC = Short-Circuit Current (three-phase). All values were calculated using the Thevenin equivalent method. Inverter-based ESS units were modeled with a maximum fault current contribution of 1.5 p.u. The maximum observed increase in short-circuit current across all buses was well below the 20% protection coordination threshold in both test systems.

Table A2: Reliability parameters for EENS calculation.

Component	Failure Rate (λ) (failures/year)	Repair Time (r) (hours)	Outage Probability ($p = \lambda \times r/8760$)
Conventional Generator	0.5	10	0.00057
PV Plant	0.3	8	0.00027
WT Plant	0.4	12	0.00055
Distribution Line (per km)	0.05	5	0.0000285

References

1. Golmohammad M, Sabzpoosh Saravi V, Alipour H, Bozorgmehri S, Bazgir M. Power management in grid-scale energy storage systems; a case study of trends. Hydrog Fuel Cell Energy Storage. 2025;12(2):105–26.
2. Mohamad F, Teh J. Impacts of energy storage system on power system reliability: a systematic review. Energies. 2018;11(7):1749. doi:10.3390/en11071749.
3. Sharma S, Niazi KR, Verma K, Rawat T. Impact of multiple battery energy storage system strategies on energy loss of active distribution network. Int J Renew Energy Res. 2019;9(4):1705–11. doi:10.20508/ijrer.v9i4.10030.g7773.
4. Shao Y, Ding R, Tian Z. An optimal configuration method for energy storage systems in distribution networks considering battery life. In: Proceedings of the 2020 IEEE 3rd Student Conference on Electrical Machines and Systems (SCEMS); 2020 Dec 4–6; Jinan, China. p. 692–7. doi:10.1109/scems48876.2020.9352260.
5. Hossain E, Faruque HMR, Sunny MSH, Mohammad N, Nawar N. A comprehensive review on energy storage systems: types, comparison, current scenario, applications, barriers, and potential solutions, policies, and future prospects. Energies. 2020;13(14):3651. doi:10.3390/en13143651.

6. Stecca M, Ramirez Elizondo L, Batista Soeiro T, Bauer P, Palensky P. A comprehensive review of the integration of battery energy storage systems into distribution networks. IEEE Open J Ind Electron Soc. 2020;12:1. doi:10.1109/ojies.2020.2981832.
7. Stecca M, Elizondo LR, Soeiro TB, Bauer P. Energy storage sizing and location in distribution networks considering overall grid performance. In: Proceedings of the 2020 IEEE Power & Energy Society General Meeting (PESGM); 2020 Aug 2–6; Montreal, QC, Canada. p. 1–5. doi:10.1109/pesgm41954.2020.9281432.
8. Massucco S, Pongiglione P, Silvestro F, Paolone M, Sossan F. Siting and sizing of energy storage systems: towards a unified approach for transmission and distribution system operators for reserve provision and grid support. Electr Power Syst Res. 2021;190(45):106660. doi:10.1016/j.epsr.2020.106660.
9. Li Y, Feng B, Wang B, Sun S. Joint planning of distributed generations and energy storage in active distribution networks: a Bi-level programming approach. Energy. 2022;245(2):123226. doi:10.1016/j.energy.2022.123226.
10. Muqbel A, Al-Awami AT, Parvania M. Optimal planning of distributed battery energy storage systems in unbalanced distribution networks. IEEE Syst J. 2022;16(1):1194–205. doi:10.1109/JSYST.2021.3099439.
11. Mohamed AAR, Best RJ, Liu X, Morrow DJ, Pollock J, Cupples A. Stacking battery energy storage revenues in future distribution networks. IEEE Access. 2022;10:35026–39. doi:10.1109/access.2022.3162587.
12. Oskouei MZ, Şeker AA, Tunçel S, Demirbaş E, Gözel T, Hocaoğlu MH, et al. A critical review on the impacts of energy storage systems and demand-side management strategies in the economic operation of renewable-based distribution network. Sustainability. 2022;14(4):2110. doi:10.3390/su14042110.
13. Wang Y, Wang H, Wagner M, Liebman A. Community battery energy storage systems for enhancing distribution system operation: a multi-objective optimization approach. In: Proceedings of the 2023 IEEE International Conference on Energy Technologies for Future Grids (ETFG); 2023 Dec 3–6; Wollongong, Australia. p. 1–6. doi:10.1109/ETFG55873.2023.10408412.
14. Su R, He G, Su S, Duan Y, Cheng J, Chen H, et al. Optimal placement and capacity sizing of energy storage systems via NSGA-II in active distribution network. Front Energy Res. 2023;10:1073194. doi:10.3389/fenrg.2022.1073194.
15. Carpinelli G, Noce C, Russo A, Varilone P, Verde P. Optimal siting and sizing of battery energy storage systems in unbalanced distribution systems: a multi objective problem under uncertainty. Int J Electr Power Energy Syst. 2024;162(2023):110316. doi:10.1016/j.ijepes.2024.110316.
16. Choobdari M, Samiei Moghaddam M, Davarzani R, Azarfar A, Hoseinpour H. Robust distribution networks reconfiguration considering the improvement of network resilience considering renewable energy resources. Sci Rep. 2024;14(1):23041. doi:10.1038/s41598-024-73928-1.
17. Naghibi AF, Akbari E, Veisi M, Shahmoradi S, Pirouzi S. Capabilities of battery and compressed air storage in the economic energy scheduling and flexibility regulation of multi-microgrids including non-renewable/renewable units. Sci Rep. 2025;15(1):24856. doi:10.1038/s41598-025-06768-2.
18. Ba-swaimi S, Verayiah R, Ramachandaramurthy VK, ALAhmad AK, Padmanaban S. Optimal planning of renewable distributed generators and battery energy storage systems in reconfigurable distribution systems with demand response program to enhance renewable energy penetration. Results Eng. 2025;25:104304. doi:10.1016/j.rineng.2025.104304.
19. Karve GM, Thakare MS, Vaidya GA. Optimal siting and sizing of battery energy storage system in distribution system in view of resource uncertainty. Energies. 2025;18(9):2340. doi:10.3390/en18092340.
20. Li J, Zhao T, Sun D, Ma J, Yu H, Yan G, et al. Multi-layer optimization method for siting and sizing of distributed energy storage in distribution networks based on cluster partition. J Clean Prod. 2025;501(1):145260. doi:10.1016/j.jclepro.2025.145260.
21. Kuraguchi S, Kaneko A, Ishii T, Yoshinaga J, Hayashi Y, Fujita N, et al. Optimal placement of grid battery energy storage systems for congestion mitigation and enhanced power-flow control considering uncertainties in photovoltaic deployment. IEEJ Trans Elec Eng. 2025;17(22):tee.70225. doi:10.1002/tee.70225.
22. Gotzias G, Stai E, Papavassiliou S. Fairness-performance trade-offs in active power curtailment for radial distribution grids with battery energy storage. Energies. 2025;18(22):5873. doi:10.3390/en18225873.
23. Jain P, Tandon A, Dubey B. Optimal placement and sizing of battery energy storage system in renewable energy system integrated distribution systems. Cureus J Eng. 2025:1–16. doi:10.7759/s44388-025-03882-9.

24. Qi H, Yan X, Kang Y, Yang Z, Ma S, Mi Y. Multi-objective optimization strategy for the distribution network with distributed photovoltaic and energy storage. Front Energy Res. 2024;12:1418893. doi:10.3389/fenrg.2024.1418893.
25. Shen F, Luo Q. A multi-objective optimization framework for optimal configuration of battery energy storage system in peak shaving and valley filling scenarios. Appl Sci. 2026;16(5):2357. doi:10.3390/app16052357.
26. Tapia-Aguilera J, Grisales-Noreña LF, Quintal-Palomo RE, Montoya OD, Sanin-Villa D. Optimizing energy storage systems with PSO: improving economics and operations of PMGD—a Chilean case study. Appl Syst Innov. 2026;9(1):22. doi:10.3390/asi9010022.
27. Xu N, Mu C, Wang K, Ma L, Liu Z. Multi-agent generalized cooperative optimization scheduling for multi-energy complementarity in microgrids. Artif Intell Rev. 2026;59(2):43. doi:10.1007/s10462-025-11354-z.
28. Zhu L. Research on multi-objective coordinated planning of distribution networks based on improved generative adversarial networks. IEEE Access. 2025;13(11):134129–42. doi:10.1109/ACCESS.2025.3592675.
29. Su H, Zhao T, Che Y, Ge L, Ma X, Zheng Y. Multi-objective site selection and capacity optimization of distributed PV energy storage in smart distribution network based on non-cooperative game. Period Polytech Elec Eng Comp Sci. 2025;69(3):318–33. doi:10.3311/ppee.40676.
30. Vijayan V, Arzani A, Mahajan SM. Enhancing operational planning of active distribution networks considering effective topology selection and thermal energy storage. iEnergy. 2025;4(2):98–106. doi:10.23919/IEN.2025.0013.
31. Iqbal H, Stevenson A, Sarwat AI. Impact analysis and optimal placement of distributed energy resources in diverse distribution systems for grid congestion mitigation and performance enhancement. Electronics. 2025;14(10):1998. doi:10.3390/electronics14101998.
32. Ohirul Qays M, Buswig Y, Hossain ML, Abu-Siada A. Active charge balancing strategy using the state of charge estimation technique for a PV-battery hybrid system. Energies. 2020;13(13):3434. doi:10.3390/en13133434.
33. Qays MO, Ahmad I, Habibi D, Masoum MAS, Mahmoud T. Addressing system strength and reliability concerns in renewable energy-based weak grids using synchronous condensers determined by hybrid GRU-classical optimization method. Sustain Energy Grids Netw. 2026;45:102111. doi:10.1016/j.segan.2025.102111.
34. Riffonneau Y, Bacha S, Barruel F, Ploix S. Optimal power flow management for grid connected PV systems with batteries. IEEE Trans Sustain Energy. 2011;2(3):309–20. doi:10.1109/tste.2011.2114901.
35. Bagherian A, Moghaddas Tafreshi SM. A developed energy management system for a microgrid in the competitive electricity market. In: Proceedings of the 2009 IEEE Bucharest PowerTech; 2009 Jun 28–Jul 2; Bucharest, Romania. p. 1–6. doi:10.1109/PTC.2009.5281784.
36. Luo X, Wang J, Dooner M, Clarke J. Overview of current development in electrical energy storage technologies and the application potential in power system operation. Appl Energy. 2015;137:511–36. doi:10.1016/j.apenergy.2014.09.081.
37. Vazquez S, Lukic SM, Galvan E, Franquelo LG, Carrasco JM. Energy storage systems for transport and grid applications. IEEE Trans Ind Electron. 2010;57(12):3881–95. doi:10.1109/tie.2010.2076414.
38. Xu B, Zhao J, Zheng T, Litvinov E, Kirschen DS. Factoring the cycle aging cost of batteries participating in electricity markets. IEEE Trans Power Syst. 2018;33(2):2248–59. doi:10.1109/tpwrs.2017.2733339.
39. Sultana B, Mustafa MW, Sultana U, Bhatti AR. Review on reliability improvement and power loss reduction in distribution system via network reconfiguration. Renew Sustain Energy Rev. 2016;66(7):297–310. doi:10.1016/j.rser.2016.08.011.
40. Saadat H. Power system analysis. Boston, MA, USA: WCB/McGraw-Hill; 1999.
41. Kumar P, Ali I, Thomas MS, Singh S. Imposing voltage security and network radiality for reconfiguration of distribution systems using efficient heuristic and meta-heuristic approach. IET Generation Trans Dist. 2017;11(10):2457–67. doi:10.1049/iet-gtd.2016.0935.
42. Qawaqzeh M, Al_Issa HA, Buinyi R, Bezruchko V, Dikhtyaruk I, Miroshnyk O, et al. The assess reduction of the expected energy not-supplied to consumers in medium voltage distribution systems after installing a sectionalizer in optimal place. Sustain Energy Grids Netw. 2023;34(6):101035. doi:10.1016/j.segan.2023.101035.
43. Data AR. IEEE Std 3006.8^{TM}-2018. New York, NY, USA: IEEE; 2018.

44. Spertino F, Chiodo E, Ciocia A, Malgaroli G, Ratclif A. Maintenance activity, reliability, availability, and related energy losses in ten operating photovoltaic systems up to 1.8 MW. IEEE Trans Ind Appl. 2021;57(1):83–93. doi:10.1109/tia.2020.3031547.
45. Maghami MR, Thang KF, Mutambara AGO, Firoozi AA, Yaghoubi E, Jahromi MZ, et al. Optimized planning of electric vehicle charging infrastructure for grid performance improvement. Discov Sustain. 2025;6(1):706. doi:10.1007/s43621-025-01522-0.
46. Shahrbejari AN, Sani MHE, Jahromi MZ, Yaghoubi E, Yaghoubi E, Maghami MR. Optimal multi-objective energy management of decentralized demand response incorporating uncertainties. PLoS One. 2025;20(7):e0328838. doi:10.1371/journal.pone.0328838.